ATMOSPHERIC ENVIRONMENT: X 5 (2020) 100049

Contents lists available at ScienceDirect

Atmospheric Environment: X

journal homepage: http://www.journals.elsevier.com/atmospheric-environment-x

Photopaper as a tool for community-level monitoring of industrially produced hydrogen sulfide and corrosion

Lourdes Vera [a,*,1], Garance Malivel [b,2], Drew Michanowicz [c,3], Choong-Min Kang [c,4], Sara Wylie [a,5]

[a] Northeastern University, 900 Renaissance Park, 360 Huntington Ave, Boston, MA, 02115, USA
[b] York University, 4700 Keele St, Toronto, ON M3J 1P3, Canada
[c] T.H. Chan Harvard School of Public Health, 677 Huntington Ave, Boston, MA, 02115, USA

ARTICLE INFO

Keywords:
Citizen science
Hydrogen sulfide
Corrosion
Community science
Environmental justice
Oil extraction

ABSTRACT

Scientific instrumentation driven by academic, military, and industrial applications tends to be high cost, designed for expert use, and "black boxed". Community-led citizen science (CLCS) is creating different research instruments with different measurement goals and processes. This paper identifies four design attributes for CLCS tools: affordability, accessibility, builds community efficacy and provides actionable data through validating a community method for monitoring the neurotoxic and corrosive gas Hydrogen Sulfide (H_2S). For $1 per sample, the semi-quantitative method provides an affordable and easily interpretable data for communities to compare H_2S concentrations and silver corrosion in their home environments to those in a major municipal sewage treatment plant.

H_2S is a leading cause of workplace injury in the U.S. and commonly found in oil and gas production, sewage treatment plants, and concentrated animal feeding operations (CAFOs). Communities neighboring such sources tend to be socio-economically marginalized with little access to scientific or political resources. Consequently, health risks and material degradation from corrosion are well studied in workplaces while community exposures are under-studied. Existing commercial H_2S detection methods are prohibitively expensive for low-income communities and often require the support of professional scientists. This paper describes a simple and inexpensive semi-quantitative H_2S measurement method that uses photopaper.

Photopaper passively measures H_2S as its silver halide layer linearly reacts with H_2S between concentrations of 30 ppb to 1000 ppb, discoloring the paper from white to brown. We develop a colorimetric scale for this discoloration for visual estimation of H_2S concentration and overall corrosion. The scale is based on comparing silver sulfide (Ag_2S) measured by Purafil Corrosion Classification Coupons (CCCs) and H_2S concentrations measured with the industry standard tool, a Jerome meter, to silver and sulfur bound to the photopaper as measured with X-Ray Fluorescence (XRF). We conduct our validation studies in a major municipal sewage treatment plant to provide real-world occupational benchmarks for comparison to community results. This community science method is affordable, accessible, designed to build collective efficacy and to create actionable data to flag the need for follow-up research.

1. Introduction

Environmental injustice and the need for community science. Research in environmental health and justice is producing new community-led citizen science (CLCS) tools, goals, and scientific communities (Bullard, 2008; Allen, 2003; Macey et al., 2014; Castner et al., 2018; Public Lab: a

* Corresponding author. Department of Sociology and Anthropology, Northeastern University, USA.
E-mail address: L.Vera@northeastern.edu (L. Vera).
[1] Lourdes Vera is a doctoral student in the department of Sociology and Anthropology at Northeastern University.
[2] Garance Malivel is an MA student at York University.
[3] Drew Michanowicz is a Post-Doctoral Researcher at Harvard T.H. Chan School of Public Health.
[4] Choong-Min Kang is a research associate at Harvard T.H. Chan School of Public Health.
[5] Sara Wylie is an Assistant Professor in the departments of Sociology and Anthropology and Health Sciences at Northeastern University.

https://doi.org/10.1016/j.aeaoa.2019.100049
Received 1 May 2019; Received in revised form 17 September 2019; Accepted 24 September 2019
Available online 30 September 2019

DIY environmental science community, 2019; Kenny et al., 2019; Liboiron, 2017; Eriksen et al., 2018). Environmental justice (EJ) research addresses the inequitable distribution of environmental hazards and benefits produced by systems of oppression such as colonialism, classism, and racism (Bullard, 2008; Pulido, 2018; Pulido, 2017; People of Color Environmental Justice Summit, 1991; Pellow, 2016). Low-income communities of color are exposed to more environmental hazards from industrial sources than higher income, majority white areas (Bullard, 2008; Agyeman et al., 2016; Clough, 2018; Nicole, 2013; Malin and DeMaster, 2016; Wilson et al., 2002). The distance of EJ communities from academic research helps produce forms of research, tools, and metrics for risk that can make these conditions harder to study (Allen, 2003; Murphy, 2006; Ottinger, 2010; Corburn, 2005; Saxton, 2015; Hess, 2016). Community environmental health complaints can be dismissed because concentrations do not exceed regulatory thresholds established in limited laboratory conditions (Allen, 2003; Murphy, 2006; Shapiro, 2015; Richter et al., 2018).[6] In response, communities and academics are developing affordable and accessible CLCS tools that research complex lived conditions of exposures, designed not for academic and occupational research, but for generating collective efficacy and valid actionable data (Allen, 2003; Public Lab: a DIY environmental science community, 2019; Ottinger, 2010; Corburn, 2005; Bandura, 1997; Bandura, 2000; Wylie et al., 2014; Matz et al., 2017).

Affordable Tools. CLCS tools need to be affordable. Academic research devices tend to be costly, state-of-the-art, and designed for ever-increasing precision in laboratory and industrial settings. Bucket brigades have pioneered work in community science by developing a CLCS alternative to Summa canisters, replacing costly spherical metal vacuum chambers that suck in and sample ambient air with sealed Tedlar bags in transparent plastic buckets that vacuum air through a foot pump (Macey et al., 2014). For a fraction of the cost, bucket samples can be pivotal in proving community exposure to environmental health risks (Allen, 2003; Macey et al., 2014; Ottinger, 2010).

Accessible Tools. CLCS tools need to be accessible to non-professionals by teaching them how measurements work and providing meaningful data. Black-boxed instrumentation that provide only numerical readouts do not educate users in how measurement devices work (Wylie et al., 2017; Latour and Woolgar, 1986; Latour, 1987). This approach encourages a deficit model of learning where communities are dependent on others to define and diagnose their conditions (Paulo, 1968; Minkler and Wallerstein, 2008). Communities have unique, experiential knowledge of environmental conditions (they smell rotten eggs, see smoke, develop a cough or a headache) (Shapiro, 2015). Similarly, all measurement devices rely in some way on analog detection, a measurable change in a reactive medium (Wylie et al., 2017). However, that reactive medium and its measurements are frequently buried within an instrument. CLCS tools that unearth the reactive medium or sample-gathering process connect more readily to embodied experiences (Public Lab: a DIY environmental science community, 2019; Liboiron, 2017; Wylie et al., 2017). For instance with bucket sampling, communities assemble transparent buckets through which they can see them vacuum in air, which increases understanding of the tool and data-gathering process (Ottinger, 2010).

Tools for Collective Efficacy. Research tools can build collective efficacy (CE), the ability of a group of people to recognize themselves as a community and act on their shared interests (Bandura, 1997, 2000). In public health, higher CE strongly correlates with reduced environmental and human health risks (Browning et al., 2008; Cohen et al., 2008; Fagan et al., 2014; Goddard et al., 2004; Sampson et al., 1997). Community exposures are inherently collective, however the consequences of exposure tend to be individual: a person develops a cough, another a headache, another's livestock falls ill. EJ work aims to gather and articulate these individual problems as part of a collective, structural issue (Allen, 2003; Brown et al., 2004, 2011). CLCS tools can support this process. For instance, in Bucket Brigades, community members work as a group to develop community goals, testing plans, and sampling strategies. This collective process draws people together differently than an engineer conducting daily monitoring at an industrial facility.

Actionable data. Community-led science often has very different immediate aims from academic science (Liboiron, 2017; Shapiro, 2015; Wylie et al., 2017). Whereas academic research often seeks to establish basic mechanisms or causal relationships, EJ-driven community science primarily addresses local environmental health risks to rapidly reduce harms (Corburn, 2005; Thomas, 2017; Wylie et al., 2017b). Thus, rather than a systematic airshed study, a few samples showing potential exposures to a vulnerable population could be sufficient for community science work seeking to prevent the expansion of a refinery (Brody et al., 2009).

Designing with these core attributes of CLCS tools: affordability, accessibility, collective efficacy and actionable data, this paper develops and validates photopaper as a tool for community identification of hydrogen sulfide (H_2S) and silver corrosion. This project began with community complaints about H_2S released during oil and gas extraction, particularly in Wyoming (WY), where companies are only required to plan for emergency accidental H_2S releases (Wylie et al., 2017; Wylie and Albright, 2014; Skrtic, 2006). In 2013, we monitored H_2S with photopaper on a WY meat goat ranch with two oil wells. The wells discharge water, produced with the oil, into three waste-pools that separate oil waste by gravity alone and release "clean" water into the riparian system. Though the ranchers complained of frequent rotten egg smells, burning eyes and noses, central nervous system dysfunction consistent with H_2S exposure, and an oil pipeline on the property ruptured due to corrosion, their concerns were routinely dismissed by state regulators (Wylie et al., 2017). Bucket sampling on their property identified 48 ppm of H_2S at the waste water discharge (Wylie et al., 2017; Thomas, 2014, 2017). The struggles of these ranchers and other EJ communities motivated our development of this photopaper tool.

Hydrogen sulfide and the need for CLCS Tools. H_2S is a leading cause of workplace injury in the United States and commonly released in oil and gas production, sewage treatment plants, and CAFOs (Skrtic, 2006; Kornblug, 2014; Finnbjornsdottir et al., 2016; Kilburn et al., 2010; Kilburn, 2012; Kilburn and Warshaw, 1995). 15–25% of U.S. oil and gas wells are predicted to contain H_2S (Skrtic, 2006). H_2S, produced by bacterial degradation of organic matter, can induce lasting physiological and neurological effects from both acute high-level exposures and low-level chronic exposures (Skrtic, 2006; Kilburn et al., 2010; Legator et al., 2001). While the human olfactory system is extremely sensitive to sulfurous compounds below many device detection limits, smell is not a reliable proxy since it can be desensitized at low concentrations or paralyzed at high concentrations (Skrtic, 2006; Kilburn and Warshaw,

[6] Research in the social studies of science have documented many problems with existing research paradigms for addressing environmental injustice. Toxicology relies on laboratory models to identify no observable effect levels (NOEL) on a chemical by chemical basis in genetically standardized organisms. NOELs are used to set threshold limit values (TLVs) below which exposures are presumed safe. Field studies then analyze whether concentrations exceed TLVs. When not exceeded, reported health issue have been dismissed rather than TLVs or toxicology being questioned (Murphy, 2006; Oreskes and Conway, 2011), this is particularly problematic for endocrine disrupting compounds with low does effects (Vogel, 2012; Wylie, 2018). Additionally there are huge lags in exposures, health problems, epidemiological studies and data (Allen, 2003; Wing, 1994, 1998). Data often fail to circulate to communities (Brody et al., 2014) and industrial influence can shape research outcomes (Richter et al., 2018; Wylie, 2018; Wing, 1994, 1998; Oreskes and Conway, 2011; Markowitz and Rosner, 2013). We accept a paradigm of research where communities must become sick in statistically significant fashions before we determine industrial systems to be harmful. There are many statistical issues with analyzing exposures to small communities that might results in many different and latent health problems (Allen, 2003; Wing, 1998).

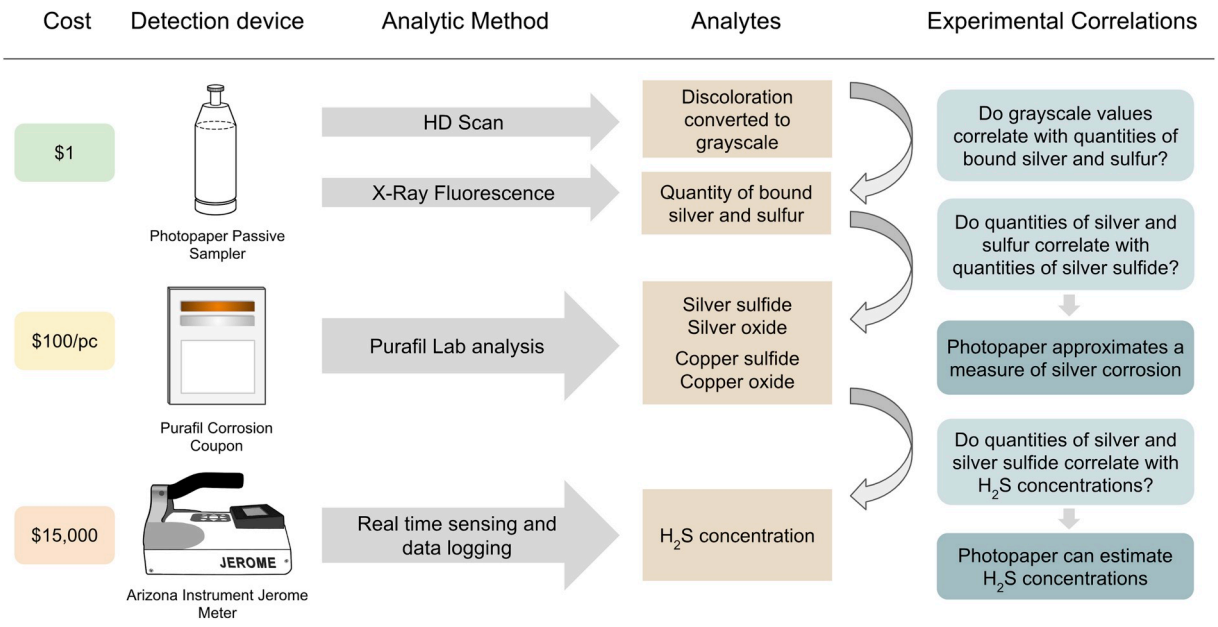

Fig. 1. Validation plan for the photopaper passive samplers.

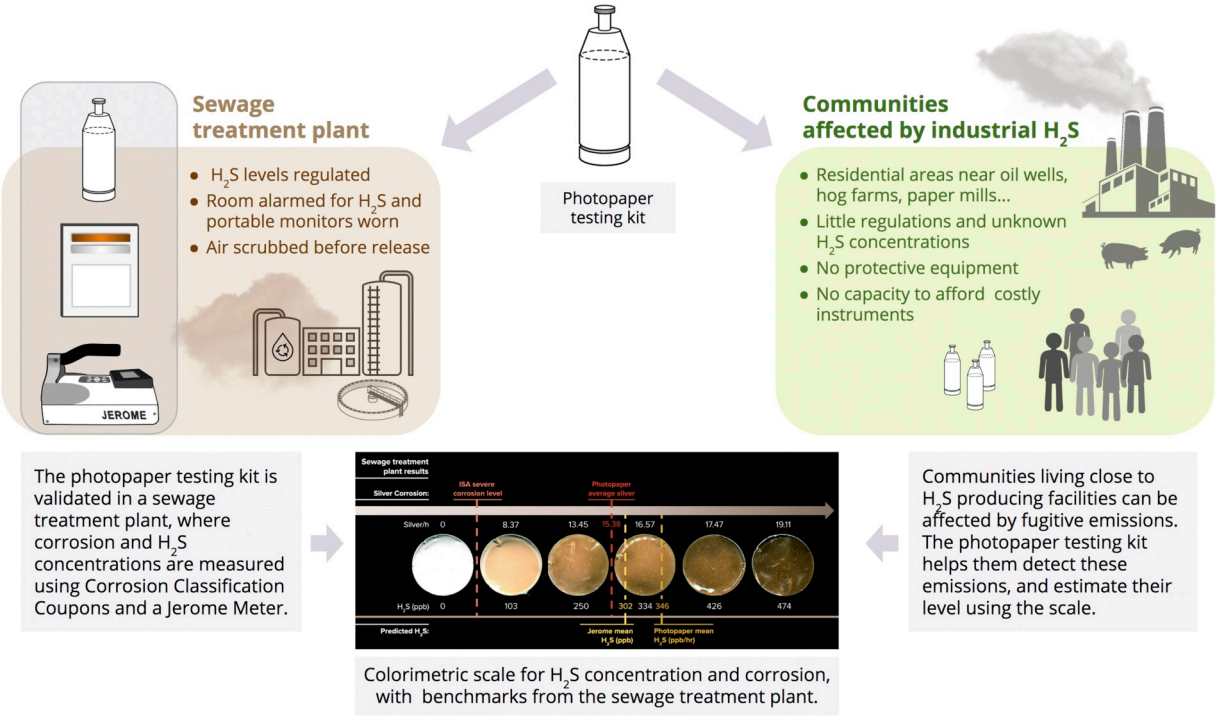

Fig. 2. Paper graphical abstract and study design.

1995). H_2S is corrosive, and corrosion comprises one of the largest single U.S. economic expenses estimated at up to 3.4% GDP or $2.5 trillion for 2013 (Koch et al., 2016). While corrosion is well-studied across industrial sectors, limited studies are available on community-level corrosion impacts in areas where reduced sulfur gases are emitted.

Recent advancements in H_2S measurement techniques include tunable diode laser spectrometry, UV absorption spectroscopy, and electrochemical cells (Carpenter et al., 2017; Rosolina et al., 2016). However, these are often not accessible to EJ communities and require the help of professional scientists. A Jerome meter, the industry standard active sampler to quantify H_2S, costs ~$15,000, plus ~$700 annually for calibration (Arizona InstrumentsLLC, 2015). Purafil Corrosion Classification Coupons (CCCs) can be used to estimate ranges of H_2S and sulfur dioxide (SO_2) based on the corrosion of cleaned strips of copper and silver, yet cost $100 per coupon and are designed for indoor use (CCC (Corrosion Classification Coupon), 2019). Passive samplers such as Sigma-Aldrich Radiello tubes can monitor chronic, low amounts of H_2S, yet in our experiences, and as documented by Venturi et al., results from these samplers have not been reliable (Venturi et al., 2016). While some multi-gas monitors exist for H_2S, they are relatively expensive and

designed for workplace exposures.

Some affordable measurement devices exist but they are purely qualitative and/or for water rather than air monitoring (Quddious et al., 2016). H_2S measurement by lead acetate tape is low-cost, reliable, low-maintenance, and relies on the darkening due to the formation of black lead sulfide (PbS), which is linearly proportional to ambient H_2S concentrations (Natusch et al., 1974). While easily interpretable, lead acetate results are strictly qualitative, have high limits of detection (e.g., 5–10 ppm), and use lead, a neurotoxin (Sanderson et al., 1966). Other colorimetric H_2S sensing methods exist for water sampling such as a disposable paper substrate utilizing copper-complex reactions accompanied with a colorimeter (Hydrogen Sulfide Test Kit, 2019).

To address these methodological barriers, we develop an affordable and accessible CLCS photopaper tool to estimate H_2S concentration and corrosion with a colorimetric scale that builds collective efficacy and provides actionable data (Wylie et al., 2017) (Fig. 1). Developed to study volcanically-produced H_2S, photopaper's layer of silver halide (AgCl) acts as a sink for ambient H_2S gas (Horwell et al., 2004; Pal et al., 1986). The AgCl in photopaper reacts with H_2S to produce silver sulfide (Ag_2S) and discolors photopaper from white to brown proportional to atmospheric H_2S concentrations (Horwell et al., 2004).[7] Horwell et al. note that the relationship between sulfide content and paper discoloration could enable estimates of ambient H_2S concentrations based on visual observation alone (Horwell et al., 2004). However, Horwell et al. quantify photopaper sulfide by eluting sulfide for subsequent quantification (i.e., quenching of the fluorescence of fluorescein mercuric acetate (FMA) by sulfide) which required hazardous compounds (e.g., sodium cyanide) and destroyed the samples (Horwell et al., 2004). To measure photopaper sulfide content without sample destruction, we employ X-Ray Fluorescence (XRF) to obtain the silver and sulfur mass on the photopaper and validate Ilford photopaper as a measure of H_2S through comparisons with Purafil Corrosion Coupons (CCCs) and an automatic gas detector utilizing thin-gold-film amperometry (Arizona InstrumentsLLC, 2015) at a municipal sewage treatment plant (Fig. 1). We illustrate that XRF can quantify sulfur on the photopaper and thereby estimate H_2S concentration based on the equation developed in Horwell et al.'s studies (Horwell et al., 2004, 2005).

Using regression models between quantitative sulfur XRF measurements of the photopaper and grayscale values, we develop a colorimetric scale for estimating H_2S concentration through visual comparison to photopaper samples. Result from this semi-quantitative scale can inform community decisions to seek further testing. By conducting our validation studies in a major municipal sewage treatment plant, we provide real-world occupational benchmarks for comparison to community results. We hope that the comparison of community results to this regulated location provides more actionable data that flags the need for further monitoring and incentivizes regulatory and industry response (Fig. 2).

2. Methods

Photopaper. Photopaper contains light-reactive AgCl suspended in a gelatin layer, which reacts with sulfur to form silver sulfide (Ag_2S):

$$H_2S + 2AgCl \rightarrow Ag_2S + 2HCl$$

Ag_2S discolors the photopaper from white to brown. We fix photopaper using a sulfur-containing fixative that washes away unreacted AgCl, leaving Ag_2S on the paper. The formation of Ag_2S is linear between 30 ppb and 1000 ppb (Horwell et al., 2004). Above 1000 ppb, the reaction becomes non-linear, and at 2 ppm, the paper saturates and turns glossy deep brown. We follow Horwell et al.'s method with a few minor adaptations (Horwell et al., 2004; Contributors from Public Lab, 2018). As Kodak Unifix is no longer available, we used Speed Fixer (RECORD Speed Fixer, 2018) in a 10% fixative solution and fix samples for 6 min, then wash them twice in cold water. Rather than placing rectangles of photopaper in film canisters, we use 35 cent canisters for passive asbestos sampling (25 mm PCM cassettes) (Asbestos Air, 2019). We replace the asbestos filter with a 27 mm circle of activated, non-light exposed photopaper cut with a McMaster-Carr 27 mm steel punch. We activate the photopaper with a 5 min submersion in a 50/50 mixture of distilled water and glycerol with five drops of Kodak Photo Flo (Kodak Photo Flo 200 - 16 oz, 2019). Canisters are then tightly capped in a darkroom. Caps are removed for sampling without exposing the photopaper to light, recapped following the sampling period, fixed in a darkroom, air dried, and then analyzed with XRF.

Photopaper scanning and conversion to grayscale. We scan all photopaper samples on a flatbed Avision book edge FB6280E scanner at 600 DPI (FB6280E, 2019). The most homogenous area of the scan is selected, cropped, and converted to standard grayscale (255-0) using GIMP, a free and open source photo-editing software. Grayscale values are inverted so 0 is lightest and darkest is 255. This numerical range is common in measuring brightness, although we reverse it (Histogram Dialog, 2019). While grayscale values might differ slightly according to the scanner and software used, we are primarily concerned with the relationship of grayscale with sulfur and silver on the photopaper as a way to illustrate semi-quantitatively that photopaper darkness correlates with H_2S levels.

XRF analysis of photopaper. To quantify silver and sulfur on the photopaper, we use energy dispersive X-ray fluorescence (EDXRF) spectrometry (XRF Analysis), a widely applied technique for elemental analysis of filter media samples (Van Meel et al., 2007, 2008). Spectra are acquired for each sample. Elemental intensities in the sample spectra are determined by spectral deconvolution, with a least-squares algorithm. The least-squares algorithm synthesizes the spectrum of the sample under analysis by taking a linear combination of elemental shape spectra along with the background shape spectrum. The coefficients of the linear combination of elemental shapes and background spectra are scaling factors, which are determined by minimizing chi-square to produce the best fit to the sample spectrum.

We conduct elemental analysis with an Epsilon 5 EDXRF spectrometer, which utilizes secondary excitation from 10 secondary selectable targets (Van Meel et al., 2007, 2008). The spectrometer employs a 600-W dual (scandium/tungsten, Sc/W) anode X-ray tube, a 100-kV generator, and a solid state germanium (Ge) detector. MicroMatter XRF calibration standard polycarbonate films (Micromatter Co., Vancouver, Canada) are used for calibration of sulfur and silver elements.

Corrosion Classification Coupons. Based on Allen et al.'s study of H_2S emissions by drywall imported from China, we collocate the photopaper samplers in the sewage treatment plant with Corrosion Classification Coupons (CCC) (Purafil Inc., Doraville, GA) (Allen et al., 2012). Designed for indoor use, CCCs quantify corrosion and corrosive gases in an environment using strips of pre-cleaned copper and silver (Purafil, Inc., 2017). CCCs are exposed for sampling then sealed into plastic sleeves and sent to Purafil for electrolytic reduction analysis to determine amounts of copper sulfide (Cu_2S), copper oxide (Cu_2O), silver chloride (AgCl), and silver sulfide (Ag_2S). CCCs measure corrosion in angstroms of thickness (maximum measurable thickness of corrosion is 20,000 Å of Ag_2S) with results normalized to a 30-day reactivity rate, based on International Society for Automation (ISA-71.04-2013) standards for electronic equipment protection (Purafil, Inc., 2017). Corrosion severity is classified by four ISA levels: mild (corrosion is not a factor in determining equipment reliability), moderate (corrosion likely to occur and to affect equipment reliability within 5 years), harsh (corrosive attack highly likely to affect equipment in less than 5 years), and severe (corrosive attack likely to cause equipment failure within 6 months) (ASHRAE, 2014; Purafil, Inc., 2017). To compare Ag_2S detected

[7] Silver halides also react to reduced sulfur compounds such as: dimethyl sulfide($(CH_3)_2S$), carbon disulfide (CS_2), carbonyl sulfide (COS), methyl mercaptan (CH_3SH) and dimethyl disulfide ($(CH_3)_2S_2$) (Horwell et al., 2005).

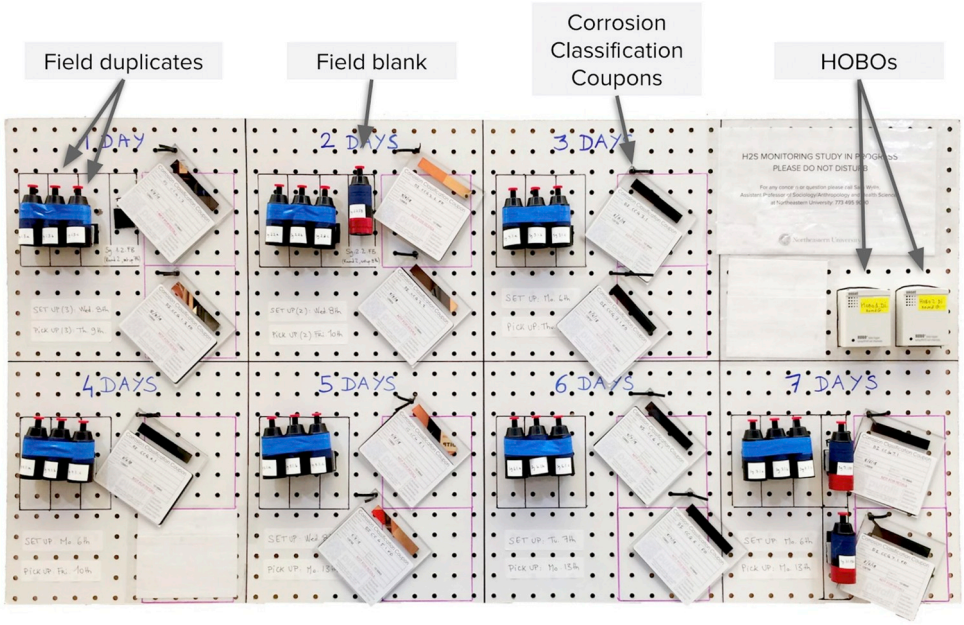

Fig. 3. Peg board used during the August 2018 validation study to collocate photopaper passive samplers and Purafil CCCs.

Time Exposed	DAY 1 - 6/8/17	DAY 2 - 6/9/17	DAY 3 - 6/10/17	DAY 4 - 6/11/17	DAY 5 - 6/12/17	DAY 6 - 6/13/17	DAY 7 - 6/14/17	DAY 8 - 6/15/17	DAY 8 - 6/16/17
	Photo sampler Corrosion Coup								
1d	Sc.A.1D (x3) 116305	pick up							
4d	Sc.A.4D (x3) 116304				pick up				
5d	Sc.A.5D (x3) 116302					pick up			
6d	Sc.A.6D (x3) 116303						pick up		
7d	Sc.A.7D (x3) 116300							pick up	
8d	Sc.A.8D (x3) 116289 (x2) Sc.A.8D.FB (116294 (FB)								pick up

Fig. 4a. Sampling plan validation study round 1 (June 2017), duplicate photopaper samples exposed at each time point.

by CCCs to photopaper samples, we adjust Purafil's 30-day estimates for time by dividing the total angstroms by 30 days, and multiplying by sampling time in hours (see Appendix 1). Our reporting of corrosion severity is based on the CCC Ag_2S only, which we compare to the calculated Ag_2S on the photopaper since Ag_2S forms on the photopaper when H_2S reacts with its silver gelatin layer. As passive samplers, CCCs also help characterize the corrosivity of the testing environment and provide benchmarks to inform our colorimetric scale.

Jerome Meter. We also collocate photopaper with an industrial standard for H_2S measurement, a Jerome® J605 Hydrogen Sulfide

Time Exposed	DAY 1 - 8/6/18	DAY 2 - 8/7/18	DAY 3 - 8/8/18	DAY 4 - 8/9/18	DAY 5 - 8/10/18	DAY 6 - 8/11/18	DAY 7 - 8/12/18	DAY 8 - 8/13/18
	Photo sampler Corrosion Coup	Photo sampler Corrosion Coup	Photo sampler Corrosion Coup					
1d	Sg.1.1 (x3) CCg.1.1 (x2)	pick up						
2d	Sg.2.1 (x3) CCg.2.1		pick up					
3d	Sg.3.1 (x3) CCg.3.1(x2)			pick up				
4d	Sg.4.1 (x3) CCg.4.1				pick up			
7d	Sg.7.1 (x3) CCg.7.1(x2) Sg.7.1.FB (x2)							pick up
6d		Sg.6.1 (x3) CCg.6.1 (x2)						pick up
5d			Sg.5.1 (x3) CCg.5.1					pick up
1d		Sg.1.2 (x3) CCg.1.2 (x2) Sg.1.2.FB	pick up					
1d			Sg.1.3 (x3) CCg.1.3	pick up				
2d			Sg.2.2.a (x3) CCg.2.2 (x2) Sg.2.2.FB		pick up			
7d	CCg.8.1.FB							pick up
7d	CCg.9.1.FB							pick up

Fig. 4b. Sampling plan validation study round 2 (August 2018), triplicate photopaper samples exposed at each time point.

Analyzer from Arizona Instrument LLC. The Jerome measures H_2S at levels as low as 3 ppb using a gold film sensor that increases electrical resistance when it reacts with atmospheric H_2S. The Jerome is calibrated yearly by the manufacturer and tested for accuracy before each field experiment using a Functional Test Module (AZI P/N: Z2600). On sampling days, the Jerome is warmed up and run with air stripped of H_2S, mercury vapor, and mercaptans with a Zero Air Filter (AZI P/N Z2600 3905). Other gases such as chlorine, ammonia, NO_2, and mercaptans may produce erroneous H_2S readings, although the manufacturer states that these interferences are rare (Arizona InstrumentsLLC, 2015). As an active sampler, the Jerome has higher specificity and accuracy for H_2S and therefore is used to assess our ability to estimate levels of H_2S with the photopaper.

Testing location. Through pilot testing, we identified the grit room as an area in the sewage treatment plant where H_2S levels routinely fall within the range of the reported photopaper sensitivity: 30 ppb to 1000 ppb. In the grit room, non-digestible materials are sorted from sewage and dropped on a conveyor belt that deposits the waste into trucks for hazardous waste disposal. Raw sewage enters primary separation tanks beneath the grit room through a series of sluices that are partially open to the air. Grit room air is monitored regularly for H_2S, and concentrations average between 200 and 500 ppb. Workers here are trained in H_2S safety, wear personal monitors, and the air is scrubbed clean before atmospheric release. We locate photopaper canisters, CCCs and the Jerome in the rear of the grit room attached to peg board (Fig. 3).

This study encompasses two successful week-long rounds of monitoring in the grit room from 6/8/17 to 6/16/17 and 8/6/18 to 8/13/18 (Fig. 4a and b). Following Horwell et al.'s initial experimental design, we sample daily over the course of eight days, picking up samples after, one, two, three, four, seven, and eight days of exposure. We are unable to pick up over weekends due to closure of the site. In the second round of testing, we place a second and third pair of samples on days two and three and pick them up on day eight to fill in those gaps. Explosion proofing in the room means there are no outlets to power the Jerome. The Jerome's internal battery life is limited, and its sensor needs external power to regenerate once saturated. During our first study, we take Jerome samples during daily pick-ups and for a 12 hour period before the filter is saturated. However, H_2S data from inside the scrubbing stacks show that H_2S levels vary diurnally based on sewage flow. Therefore, we do not include the June 2017 data in our comparisons to photographic paper measurements. During our second round in August 2018, we employ an external battery pack (Arizona Instrument 990-0214, $555) along with pre-charged internal batteries to extend the Jerome sampling time from 12 h to 96 h. We find during the first round that CCCs reach saturation much faster than expected. Therefore, we reduce the sampling time to seven days and add additional one, two, and three day samples in the second round.

Quality Control and Quality Assurance. Each passive sampling method has at least 10% blanks and duplicates. We use the Wilcoxon-rank sign test to assess the variance between duplicate photopaper and variance among the blanks, finding that none of the blanks differed significantly from 0. We quantify the limit of the photopaper blank based on the blank mean XRF silver and sulfur results for each location and testing round, which are reported in Appendix 1.

We encounter QC issues with some CCC duplicates. Since 20%–30% of CCCs duplicates can differ by more than a factor of two (Han et al., 2019), we remove a CCC pair (6 day CCC sample from August 2018) as it differs from its duplicate by more than a factor of two (4691 Å of Ag_2S compared to 11345 Å). One blank from August 2018 reports Ag_2S more than double the other blank and is excluded. Additionally, samples from days six and seven in August 2018 show lower corrosion than samples from days 1–5. An outlier analysis of the blank-adjusted Ag_2S, for the six (4036 Å) and seven day (5329 Å) samples shows they fall more than 2.5 standard deviations (SD = 4518.18 Å) below the blank adjusted mean of 15,218.86 Å. According to the manufacturer, as CCC reach their upper

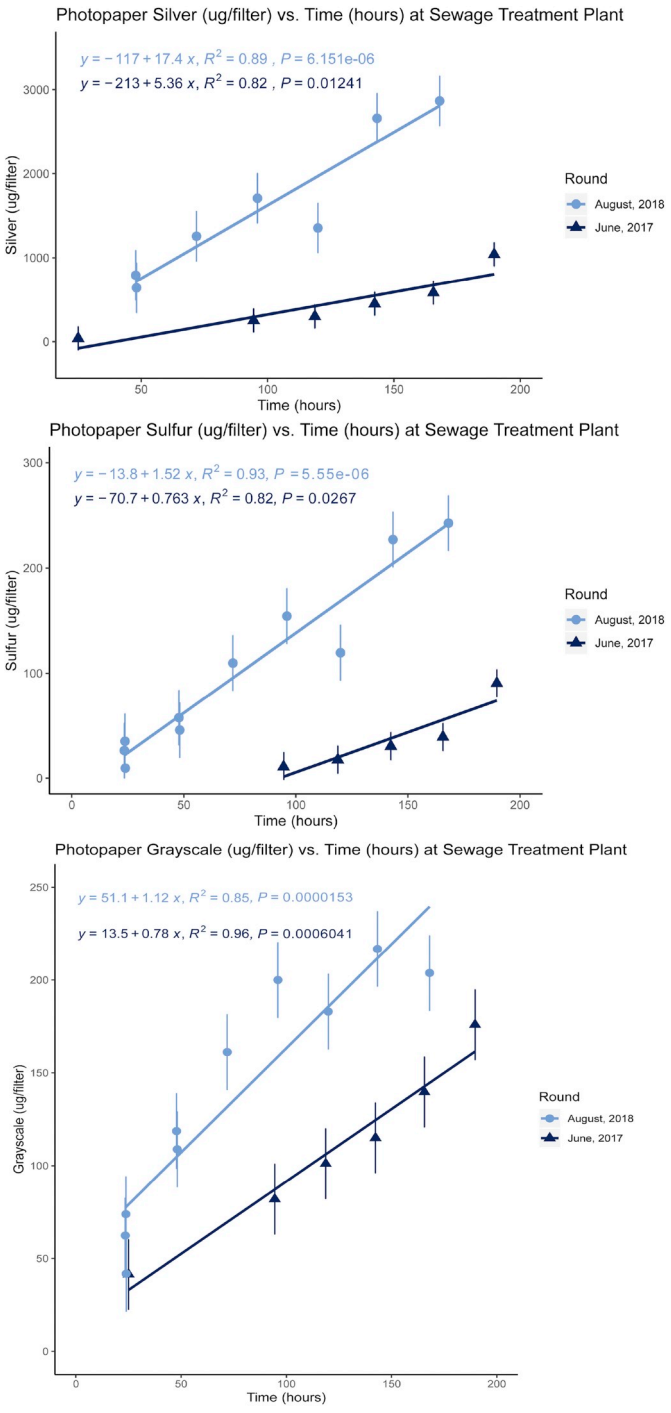

Fig. 5. Silver, sulfur, and grayscale preservation over time (in hours) by photopaper samplers during June 2017 and August 2018 validation studies at the Sewage Treatment Plant grit room.

limit of detection, the layer of corrosion can grow so thick that it flakes off. We hypothesize this occurred for day 6–7 CCCs. For these reasons, we remove CCCs 6.1 and 7.1 from our analysis. We find it important to publish the CCCs QA/QC issues to inform others using this method. We retain the remaining CCC data as reliable because duplicates for days 1–5 and 7 were consistent, a blank was blank, there is a physical explanation for the lower corrosion reported on days 6 and 7, the CCC corrosion consistently increases over days 1–5 , and all CCCs report severe corrosion by the ISA scale. Therefore, the accuracy issues are in the precise severity of corrosion rather than the overall ISA

Table 1
Sewage treatment plant rounds August 2018 and June 2017 with calculated Photopaper H_2S concentrations in ppb/hr based on XRF sulfur mass and the Silver–Sulfur reaction constant established by (Horwell et al., 2004) compared to Jerome averages per hour.

Round	Time (hours)	Sulfur (μg/filter)	S Mean of the Blank (μg/filter)	Blank-Adjusted S (μg/filter)	Predicted Total H_2S (ppb)	Predicted H_2S per Hour (ppb/hour)
June 2017	25.05	82.55	85.0939	-2.55	-715.67	-28.57
	94.50	96.03	85.0939	10.94	3071.73	32.51
	118.72	102.75	85.0939	17.66	4959.78	41.78
	142.37	115.61	85.0939	30.52	8571.88	60.21
	165.62	124.37	85.0939	39.27	11030.88	66.60
	189.67	175.72	85.0939	90.63	25456.73	134.22
August 2018	23.90	102.16	92.56	9.60	2695.42	112.78
	23.47	118.95	92.56	26.39	7412.35	315.87
	23.77	127.77	92.56	35.21	9890.65	416.16
	48.17	138.42	92.56	45.86	12881.96	267.45
	47.83	150.24	92.56	57.68	16201.34	338.70
	71.90	202.39	92.56	109.83	30849.15	429.06
	96.00	246.98	92.56	154.42	43374.09	451.81
	119.92	212.20	92.56	119.64	33605.67	280.24
	143.32	319.63	92.56	227.07	63780.96	445.04
	168.08	335.24	92.56	242.68	68165.01	405.54

Table 2
Deaver photopaper H_2S concentration sample estimates.

Round	Photopaper ID	Time (hours)	S (μg/filter)	S Mean of the Blank (μg/filter)	S Blank-Adjusted (μg/filter)	Predicted H_2S (ppb)	Predicted H_2S per Hour (ppb/hour)
July 31-August 7, 2013	D14b	168.00	88.40	100.95	-12.54	-3523.63	-20.97
	D13b	168.00	87.50	100.95	-13.44	-3776.15	-22.48
	D12b	168.00	82.34	100.95	-18.61	-5226.75	-31.11
	D17b	168.00	80.40	100.95	-20.55	-5771.94	-34.36
	D18b	168.00	76.44	100.95	-24.51	-6883.24	-40.97
	D1b	168.00	97.04	100.95	-3.91	-1098.41	-6.54
	D2b	168.00	96.68	100.95	-4.27	-1199.73	-7.14
	D3b	168.00	122.21	100.95	21.26	5972.97	35.55
	D5b	168.00	141.36	100.95	40.41	11350.91	67.56
	D7b	168.00	101.32	100.95	0.37	104.53	0.62
	D8b	168.00	89.75	100.95	-11.19	-3144.10	-18.71
	D4b	168.00	355.81	100.95	254.86	71585.73	426.11
	D15b	168.00	94.72	100.95	-6.22	-1748.16	-10.41
July 31- August 22, 2013	D12c	528.00	85.98	100.95	-14.97	-4205.53	-7.97
	D13c	528.00	91.11	100.95	-9.84	-2762.94	-5.23
	D14c	528.00	137.32	100.95	36.37	10215.51	19.35
	D15c	528.00	169.44	100.95	68.50	19239.30	36.44
	D16ic	528.00	104.84	100.95	3.89	1093.61	2.07
	D17c	528.00	85.39	100.95	-15.56	-4369.57	-8.28
	D1c	528.00	102.43	100.95	1.48	416.54	0.79
	D2c	528.00	194.13	100.95	93.18	26172.41	49.57
	D3c	528.00	731.21	100.95	630.26	177031.20	335.29
	D4c	528.00	545.98	100.95	445.03	125003.20	236.75
	D5c	528.00	250.43	100.95	149.48	41986.17	79.52
	D6c	528.00	452.34	100.95	351.39	98700.55	186.93
	D7c	528.00	373.81	100.95	272.86	76641.99	145.16
	D8ic	528.00	94.80	100.95	-6.15	-1727.23	-3.27

classification.

Temperature and Humidity. We use two Onset HOBO® U12-013 Temperature/Humidity and External Input Loggers to measure temperature and humidity. The average sewage treatment plant humidity in June 2017 is 59% and the average temperature is 72 °F. The average humidity in August 2018 is 70.8% and the average temperature is 78 °F (Appendix 2). Horwell et al. do not report significant temperature and humidity influences on the photopaper in their two field studies (Horwell et al., 2004, 2005). Oxygen and humidity can impact silver corrosion (Horwell et al., 2005; Kim, 2003; Yang et al., 2007), however, it is unclear how well this applies to photopaper where the silver is embedded in a gelatin layer. The Jerome is reliable within this temperature and humidity range. High relative humidity accelerates CCCs corrosion, particularly for copper. Above 50% of relative humidity, the corrosion severity can rise by one classification level per 10% humidity increase (ASHRAE, 2014; Purafil, Inc., 2017). Silver corrosion is less sensitive than copper to variations in temperature and humidity. We do not consider Purafil's copper corrosion classification because of copper's sensitivity to humidity and temperature.

Statistical Analysis. We used R software version 3.5.3 through RStudio Version 1.1.463 for statistical analyses. We calculate descriptive statistics, including the minimum, maximum, median, mean, and standard deviation for all parameters. All photopaper and CCC samples are adjusted by the mean of the blank for the respective testing round and location. Pearson correlations between the photopaper silver and sulfur, CCC Ag_2S, and grayscale are derived using simple linear regression. The p-values for these regressions are statistically significant at an alpha value of 0.05.

To compare CCCs and photopaper, the projected 30-day Ag_2S CCC values received from Purafil are converted to aggregate Ag_2S values for the sampling period. Blank-adjusted silver and sulfur measured from XRF are then added to estimate photopaper Ag_2S. These Ag_2S values are log-transformed and correlated in a linear regression.

To compare Jerome measurements to predicted photopaper H_2S, we

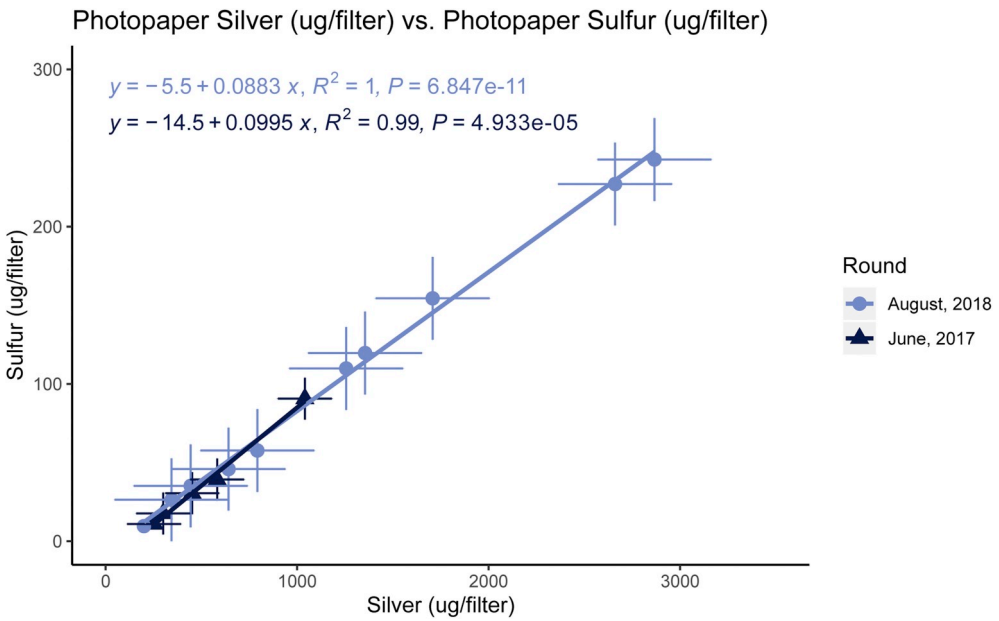

Fig. 6. Linear regression between Silver and Sulfur detected on photopaper with XRF from June 2017 (light blue points) and August 2018 (dark blue points) sewage treatment plant validation studies. (For interpretation of the references to color in this figure legend, the reader is referred to the Web version of this article.)

use Welch's T-test to test the variance in the means.

Development of the Corrosion and H_2S Concentration Colorimetric Scale. We estimate photographic H_2S concentration based on the quantity of sulfur detected with XRF and Horwell et al.'s calculation of the relationship between sulfide uptake rate (U, having units μg cm^{-2} h^{-1}) and H_2S concentration (C, having units ppb), such as $U = 6.218 \times 10^{-5} C$ (Horwell et al., 2004). The S and Ag values from each sample are blank adjusted by subtracting the mean of field blanks' S values from the respective rounds. Blank-adjusted S values are divided by the sample area (57.256 cm^2) to obtain the S per area, which is then divided by the sulfide uptake rate calculated in Horwell (0.00006218 ppb/cm) (Horwell et al., 2004). This concentration estimation based on the relationship between sulfur mass and sulfide uptake rate is divided by the number of hours the sample is deployed to generate H_2S concentrations in ppb per hour (Table 1). We arrange photopaper by increasing discoloration and H_2S concentration to form an H_2S colorimetric concentration scale. Using paired photopaper and CCC data, we also correlate discoloration with corrosion severity based on the ISA scale. The result is a photopaper colorimetric scale for H_2S and silver corrosion (see Table 2).

Field Sampling in Deaver, Wyoming. Qualitative results of field photopaper sampling conducted from July 31-August 22, 2013 on a ranch in Deaver, WY motivate this study (Wylie et al., 2017; Thomas, 2014). In these studies, photopaper is cut into rectangles and placed in tubes of black plastic. Testing locations are identified with the ranchers around the oil well and waste ponds where they routinely smell H_2S. Samples are placed where feasible as their goats graze in the pastures surrounding the oil well and waste ponds. Samples are left for one and three weeks, uncapped and open to the air but not the light, then recapped and shipped to Northeastern University to be fixed following the above protocol. We report the full design in a previous publication (Wylie et al., 2017). In this paper, we analyze the samples using XRF and locate them on our colorimetric scale.

3. Results and discussion

Analysis of Photopaper with XRF. First, we analyze the correlations between photopaper S and Ag preservation during the June 2017 and August 2018 sewage treatment plant studies (Fig. 5). Both studies show a statistically significant linear correlation between Ag, S, and grayscale. August 2018 samples have higher levels of Ag, S, and grayscale compared to June 2017. This is probably due to higher ambient H_2S concentration in the grit room during the extended heat wave prior to sampling in 2018. In August 2018, we see stronger correlations among these variables over time: Ag and S vs. T $R^2 = 0.93$ and grayscale $R^2 = 0.85$ compared to June, Ag v. Time $R^2 = 0.82$, S v. Time $R^2 = 0.75$, and grayscale v. Time $R^2 = 0.96$ (Fig. 5). All correlations are statistically significant at an alpha of 0.05.

These results show that as time increases, Ag and S on the photopaper detected by XRF increaseconsistently with continued H_2S exposure. During the June 2017 testing, the relationship is slightly less linear than the August 2018 study. We hypothesize that this is due to the photopaper detection limit at lower H_2S concentrations, which Horwell et al. approximate at 30 ppb (Horwell et al., 2004).

Additionally, we convert the discoloration of the photopaper to grayscale and see a strong, positive correlation between level of discoloration and exposure time (August 2018 $R^2 = 0.96$ and June 2017 $R^2 = 0.85$). This suggests that through a semi-quantitative analysis, grayscale may be used to estimate H_2S concentration without the use of XRF.

Next, we analyze how Ag and S correlate by plotting XRF measurements for June 2017 and August 2018. There is a strong, statistically significant positive correlation ($R^2 = 0.99$) between the two elements (Fig. 6). Ag and S in μg strongly, positively correlate ($R^2 = 0.99$ for August 2018 and $R^2 = 1$ for June 2017). The relationship is statistically significant (p-value = 6.89e-12). Of the other 72 elements detected by XRF, magnesium, aluminum, cobalt, bromine, and lead show similar positive correlations with time. As Ag increases, S increases proportionately, consistent with Ag on the photopaper being bound to S in the form of Ag_2S as predicted with H_2S exposure. The line of best fit with slopes of 0.0883 for August 2018 and 0.094 for June 2017 deviate from the ideal ratio of Ag and S predicted by their molecular weight (a line with slope of 0.149 = the atomic weight of S (32.06) divided by two times the atomic weight of Ag (107.87)). This difference is likely due to the presence of other gases in the grit room that are moderately corrosive to Ag, particularly ammonia and potentially ozone, which would increase the amount of Ag on the photopaper but not the amount of sulfur. These gases are not monitored in the grit room nor can they be easily assessed by XRF (Leygraf et al., 2016; Rice et al., 1981; Hamoda, 2006). Therefore, we use the S concentration and not the Ag to calculate

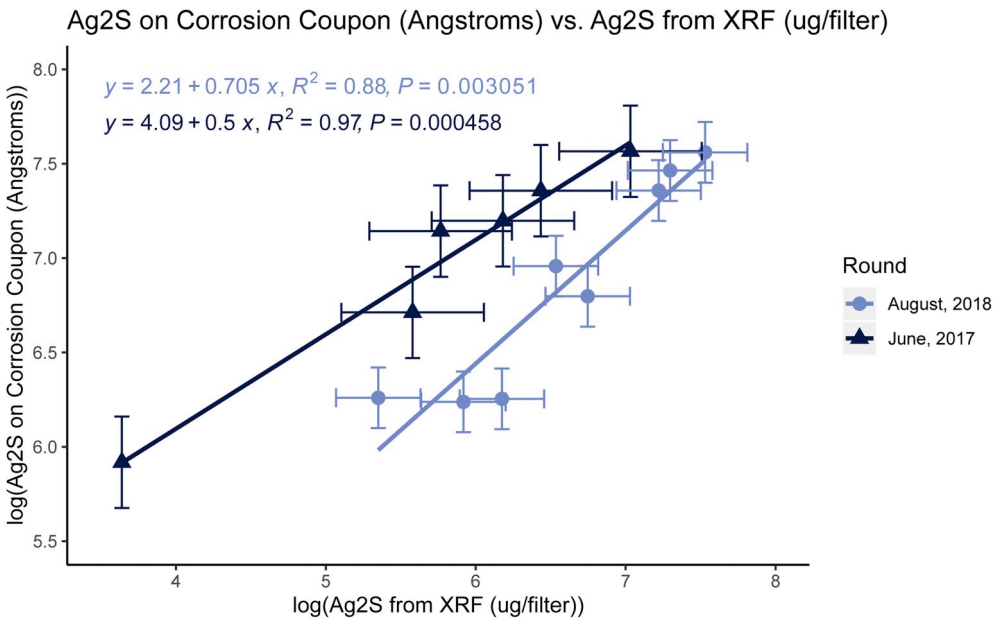

Fig. 7. Log-transformed XRF Silver from photopaper by time vs. log-transformed silver sulfide by time from CCCs across two separate sampling campaigns at a public sewage treatment plant.

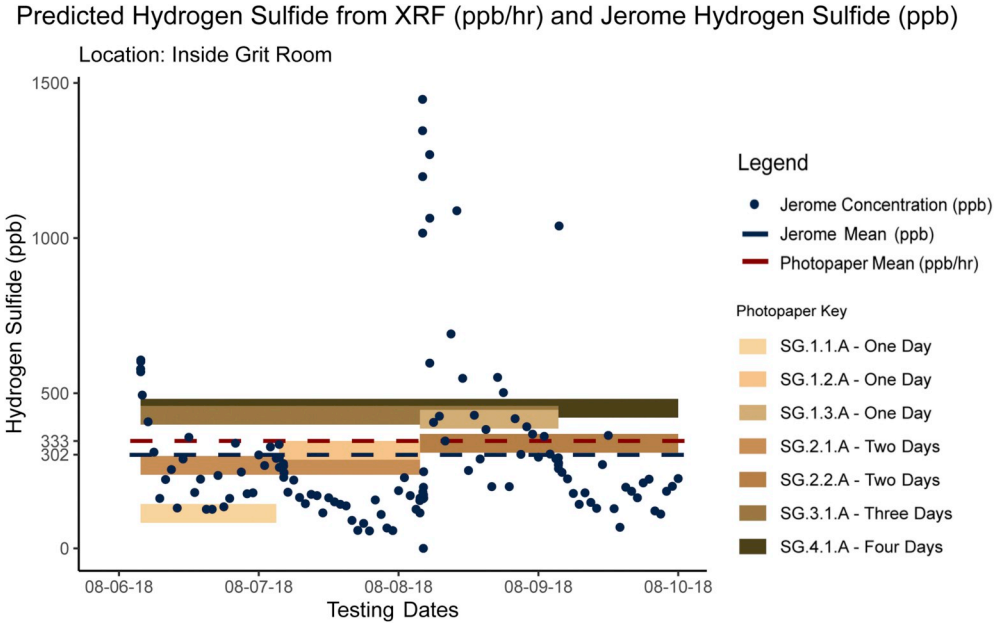

Fig. 8. This diagram compares estimated H_2S concentrations detected by photopaper (based on sulfur mass detected by XRF) and Jerome measurements taken hourly. The photopaper measurements are colored according to the actual color of the photopaper. (For interpretation of the references to color in this figure legend, the reader is referred to the Web version of this article.)

H_2S concentrations. We are investigating the use of X-ray photoelectron spectroscopy (XPS) to analyze the composition of Ag compounds.

We then calculate H_2S concentrations detected by the photopaper from the S detected with XRF using the linear uptake rate and equation constant developed by Horwell (Horwell et al., 2004)(Table 1).

Comparison of Photopaper to Reference Methods. First, we compare photopaper Ag and S XRF measurements to CCCs. We compare time and blank-adjusted Ag_2S detected on the CCCs to the sum of the blank-adjusted Ag and S measurements detected by XRF on the photopaper (Fig. 7). We log transform the data as the scales and units differ by an order of magnitude (CCC Ag_2S (angstroms) vs. photopaper (μg/filter)). This comparison shows a strong, statistically significant positive correlation at $R^2 = 0.97$ ($p = 0.000458$) for June 2017 testing and $R^2 = 0.88$ (0.0005116) for August 2018. All p-values are significant at <0.05. All CCCs paired with photopaper with an estimated 50 ppb of H_2S or above are classified as severe corrosion by the ISA scale based on Ag_2S accumulation.

Next, we compare the estimated photopaper H_2S concentrations to the Jerome meter measurements for August 2018 (Fig. 8). The Jerome samples hourly for four days resulting in 132 Jerome readings compared to ten photopaper samples. Our paired *t*-test of the Jerome measurements and photopaper H_2S concentrations provides a p-value of 0.29, suggesting the means of the two datasets are not significantly different.

The median predicted photopaper H_2S for August 2018 for the first four days when the Jerome was actively sampling is 338.7 ppb/hr and the mean 333.12 ppb/hr with a standard deviation of 117.88 (Fig. 8).

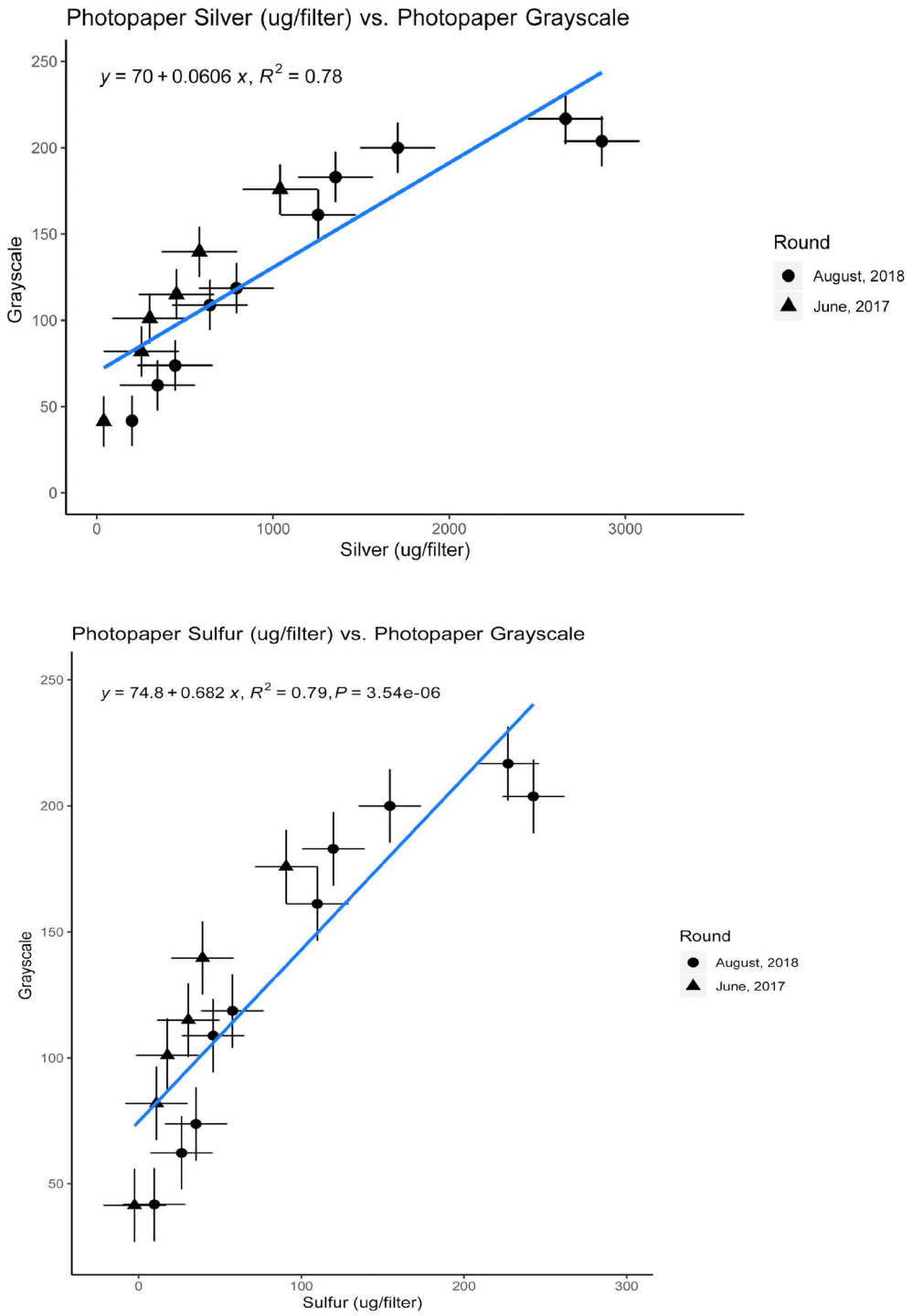

Fig. 9. Sewage treatment plant photopaper samples from June 2017 and August 2018 testing Grayscale values and silver and sulfur per area detected by XRF.

The average concentration detected by the Jerome is 301.54 ppb and the median of 223.5 ppb with a standard deviation of 260.83 ppb. These large differences in standard deviation and median can be attributed to differences in sampling durations and sample sizes. The Jerome actively samples air at one point in time while the photographic provides a passive measure over time. The Jerome measurements show a wide range of H_2S concentrations from 0 to 1447 ppb. The photopaper ranges from 112.779 ppb/hr to 451.8134 ppb/hr. Despite these differences in sampling time, the average Jerome measurement (301.54 ppb) and photopaper average (333.12 ppb/hr) are close and within each other's standard deviations. Fig. 8 compares these measurements and shows the sampling tools' inherent differences. The active Jerome sampling shows the fluctuating H_2S concentrations in the environment. The photopaper predicted hourly H_2S concentrations are generally higher when the Jerome-measured H_2S concentrations are higher. When Jerome measurements are lower, the photopaper generally reports lower hourly average values. The chart shows the photopaper mean is close to the Jerome mean as both cut across the plot in the center of where most of the measurements lie.

Based on these strong comparisons of photopaper measurements to the Jerome meter and CCC reference methods, we conclude that the photopaper is a reliable method for detecting H_2S in a field environment where concentrations fluctuate and other corrosive gases may be present and develop a colorimetric scale for visually estimating H_2S and

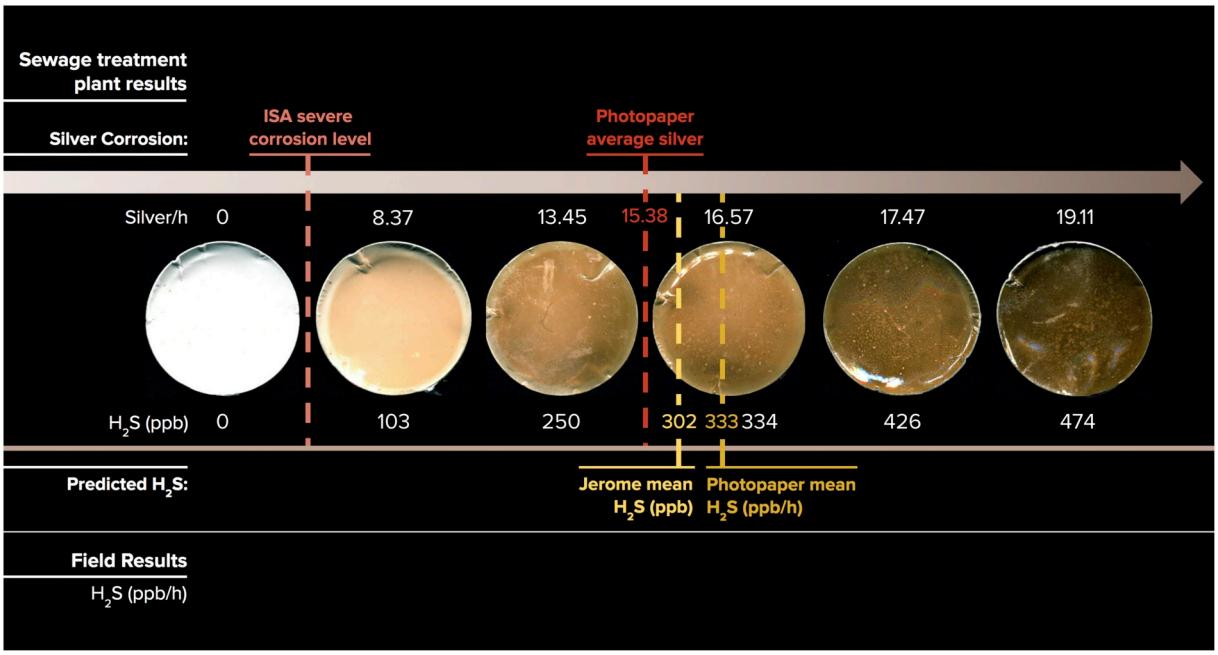

Fig. 10. Colorimetric scale from August 2018 Sewage Treatment plant testing. Note that the Jerome average is from four days of sampling and not seven.

corrosion levels using photopaper.

Development of a Colorimetric Scale for Photopaper H_2S Concentration. First, we assess whether photopaper discolors proportionately to Ag and S detected over time by scanning the photopaper, converting the scans to grayscale and comparing them to Ag and S mass per area as measured with XRF (Fig. 9). We find a moderately strong positive correlation between both Ag and grayscale ($R^2 = 0.78$) and a moderately strong correlations between S and grayscale ($R^2 = 0.79$), suggesting that discoloration is due to the presence of Ag_2S and that a colorimetric scale or grayscale could be used to estimate H_2S concentration.

We visually arrange the photopaper by shade of brown and find that Ag and S increase across the samples. Additionally, the corrosion and Ag_2S detected with the CCCs increase with photopaper discoloration. On that basis, we design a colorimetric scale for visually approximating both H_2S concentration and corrosion (Fig. 10). The scale is made with photopaper samples from the August 2018 study, and the data informing the scale can be found in Appendix 3. We add four benchmarks to the scale: the average grit room H_2S concentration, estimated by photopaper for days 1–4 (333.12 ppb); the average silver mass detected by photopaper for days 1–4 (15.38 ppb/hr); and the average H_2S concentration obtained through Jerome meter sampling for the first 4 days (301.54 ppb). Including these four benchmarks reveals a fundamental problem of measurement rather than obscuring it with a single simplified average. They show how three different detection methods can vary based on their uptake rates, reaction and analytic method in the same location. Physically speaking, there is no "average air concentration," rather there are continuous fluctuations across a relatively standard range. Thus, reporting, analyzing, or judging an environment against a single average or TLV in an effort to determine whether the environment is unsafe is to make an inductive logical error and to act as if mathematical constructions are physical realities. Reporting these four benchmarks reveals this problem to the user and allows them to determine which threshold is most relevant.

We add one further benchmark; the threshold at which the CCCs report severe corrosion. Concentrations of 50 ppb of H_2S and above recorded by CCCs are reported as 'severe corrosion' levels. All of our photopaper samples in the scale (indicated in Fig. 10) exceed 50 ppb, therefore any degree of photopaper discoloration on this scale correlates with severe corrosion by the ISA standard.

Using these benchmarks, community members can compare results on their property directly to a space where H_2S is routinely monitored and regulated. They can also estimate whether electrical and other metal equipment might be vulnerable to severe corrosion. Revealing the averages for three different detection methods illustrates that methods of detection can produce different results and all be valid measures. It also illustrates the artifice of using TLVs *or single averages as inviolate benchmarks of risk* (Murphy, 2006).

Pilot Field Test of Photopaper and Colorimetric Scale. We test the colorimetric scale with data from the 2013 Wyoming research that inspires this study and we analyze all the retrieved samples with XRF. Deaver samples are placed in pairs, with one photopaper canister of each pair picked up after eight days and the remaining canister picked up after 23 days based on the sampling strategy used by Howell et al. (Horwell et al., 2005) (Fig. 11a). Numerous samples are lost after being placed in fields actively grazed by goats. Additionally, the photopaper is placed in light-proof black plastic tubes rather than the asbestos canisters used in our validation study.

Visual assessment of the photopaper after eight days showed discoloration at D4 and D5 by the discharge canal where gravity cleaned wastewater is discharged (Fig. 11b). Discoloration is also apparent at locations D3, D4 and D5 by the discharge canal and D6 and D7 after 23 days. Locations D6 and D7 are in a patch of bushes that the ranchers feel were hydrated by wastewater leaking into the soil from the unlined waste pits and like D8 downwind of the waste pits. The ranchers took bucket samples on the property and recorded grab sample concentrations of 4.4 and 48 ppm of H_2S at the discharge canal (Wylie et al., 2017; Thomas, 2017). They did not sample close to points D6 and D7.

We then compare scans of Deaver samples to the colorimetric scale (Fig. 11d). Placing the samples by eye, the discoloration of the eight day samples approximately align with the XRF H_2S concentration prediction. However, the 23-day samples do not align well with the scale based only on discoloration (Fig. 11d). As discoloration depends on both time and concentration, the 23-day samples are very dark due their long exposure at relatively low H_2S concentrations. However, our colorimetric scale works reasonably well for short term exposures such as seven to eight days (because those time periods are close to those of our validation study), while for longer time exposures, the scale needs to be organized by exposure time and concentration.

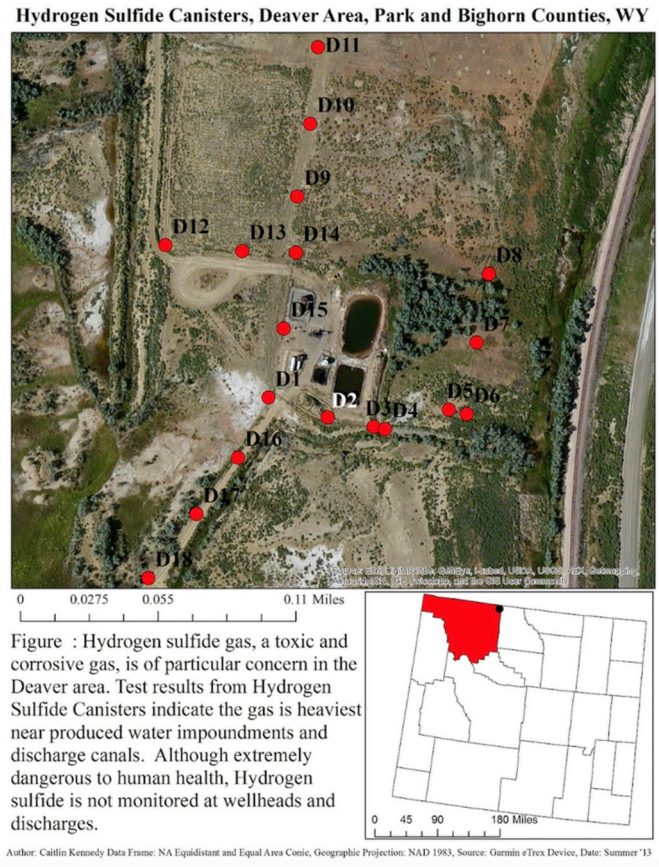

Figure : Hydrogen sulfide gas, a toxic and corrosive gas, is of particular concern in the Deaver area. Test results from Hydrogen Sulfide Canisters indicate the gas is heaviest near produced water impoundments and discharge canals. Although extremely dangerous to human health, Hydrogen sulfide is not monitored at wellheads and discharges.

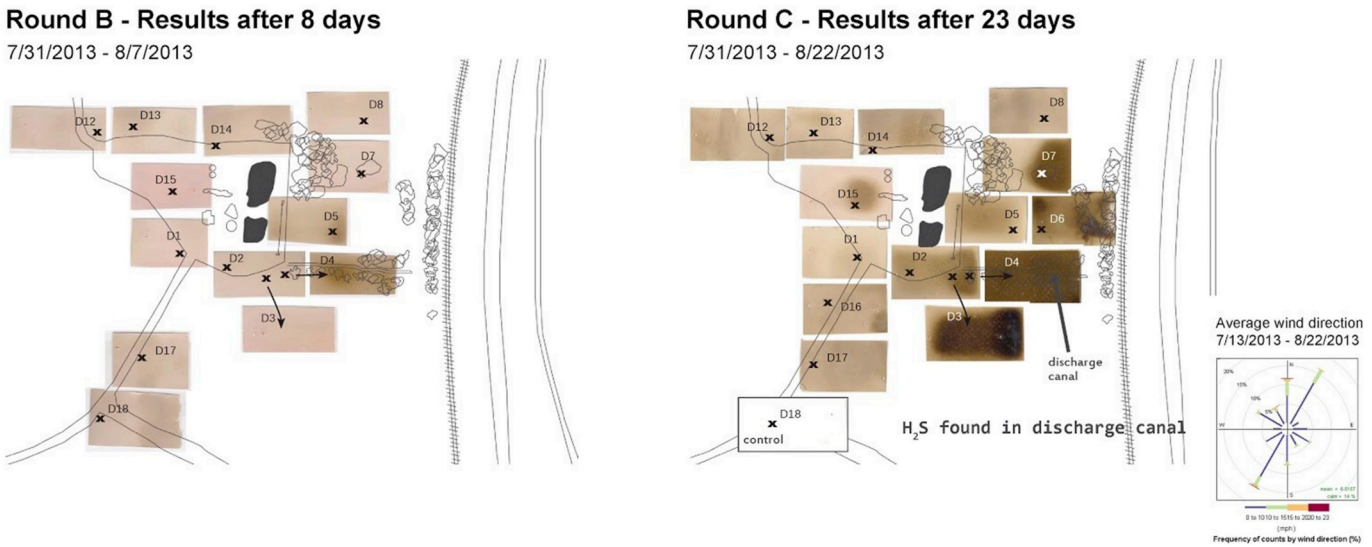

Fig. 11. (a). Testing locations on a ranch in Deaver Wyoming (From Wylie et al., 2017, republished with permission). (b). Photopaper results from Deaver (2013) testing after 8 and 23 days of exposure respectively. The strongest discoloration is seen at the point of waste discharge into the riparian system and along the discharge canal. Samples D9, D10, and D11 are compromised due to trampling by goats. Image Credit: Megan McLaughlin. Considering that six years has elapsed since this first study, we are surprised to see a strong positive correlation between silver and sulfur on the samples ($R^2 = 0.93$) (Fig. 11c). The XRF results and the estimated H_2S concentrations correlate well with the discoloration visible on the photopaper strips showing H_2S levels around the discharge canal of 223.26 ppb/hr and 317.52 ppb/hr (Fig. 11d) and the highest average concentration at location D4 (by the discharge canal) of 363.66 ppb/hr after 1 week, which is above the average photopaper concentration detected in the Grit room. (c). The 2013 Deaver samples are analyzed using XRF, showing a strong positive correlation for 11 locations. (d). Deaver photopaper concentrations and scan comparisons to colorimetric scale. The numbers inside the Deaver sample images are the H_2S concentrations calculated from XRF sulfur in ppb/hr. Note that the Jerome measurements are in ppb and have only been taken over a four day period.

4. Conclusion

Building on work by Horwell et al. (2004, 2005), we validate photopaper as a community-led citizen science (CLCS) method for detecting H_2S and corrosion by comparing to two reference methods, CCCs and the Jerome meter, for sources other than volcanoes, including sewage treatment plants and oilfield wastes. We argue that CLCS tools, in addition to being accurate, need to be affordable, accessible, build collective efficacy and create actionable data.

XRF analysis can quantify H_2S detected by photopaper. XRF is a reliable

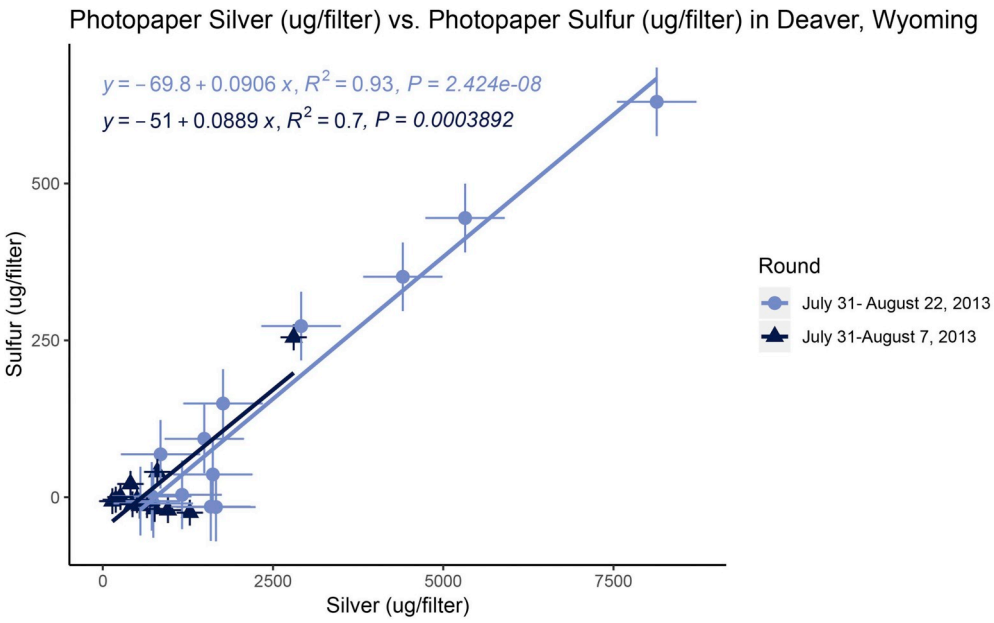

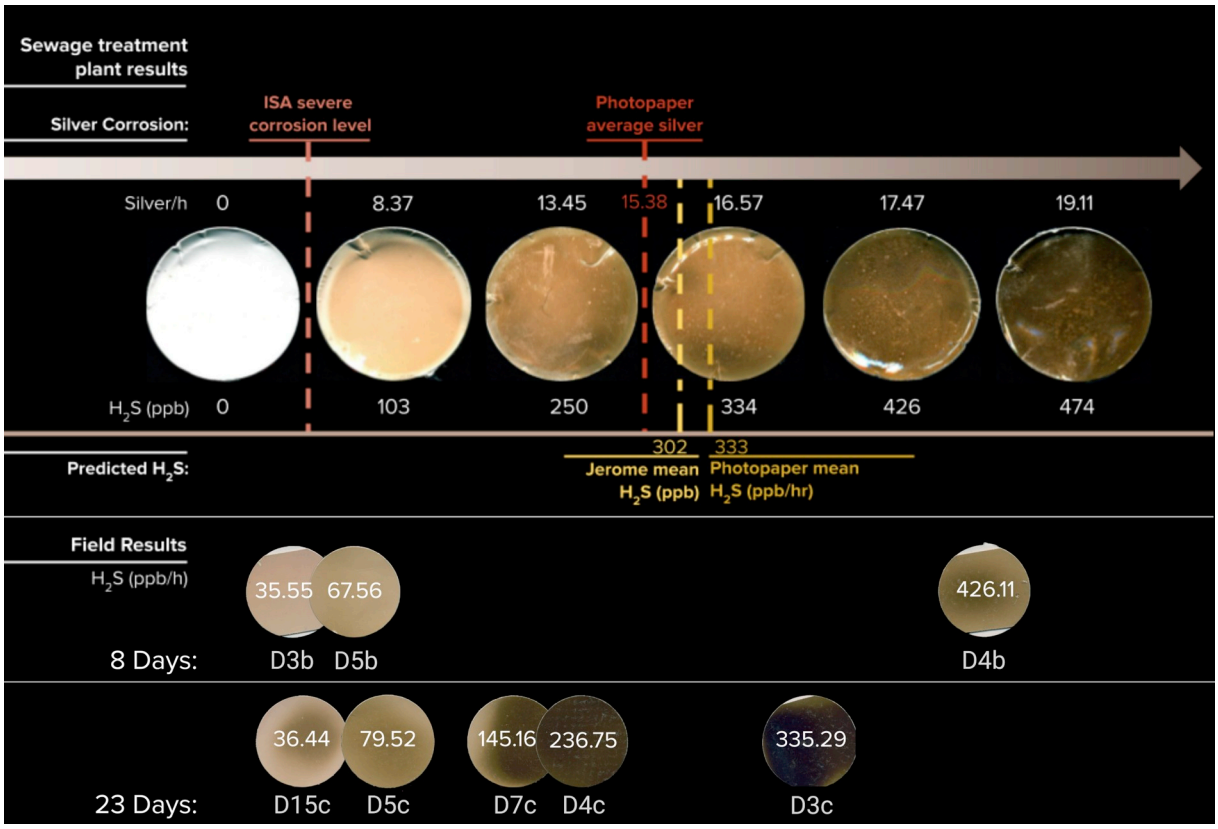

Fig. 11. (*continued*).

method for analyzing silver and sulfur adhered to the photopaper, given the comparable CCC Ag_2S concentrations and comparison with the Jerome meter. XRF analysis can compliment the CLCS photopaper method to quantify the H_2S concentration based on Horwell et al.'s initial equation.

Photopaper compares well to reference methods CCC and Jerome. Based on comparison to two reference methods (the Jerome meter and CCCs) and one direct measurement technique (XRF), we confirm that photopaper can reliably measure ambient H_2S concentrations as indicated by the strong positive correlations between Ag_2S and H_2S concentration detected by photopaper, CCCs and comparison to Jerome data.

Limitations. The sampling location and instrument battery life constrain our Jerome data. We aim to continue the comparison to these reference methods in further community testing contexts. Also, we conducted monitoring in a relatively limited H_2S concentration range (30 ppb–500 ppb). We aim to repeat our studies at closer to 1000 ppb, the expected linear photopaper uptake limit.

Affordability and Accessibility. Compared to other available methods, photopaper at ~$1 per canister is a very affordable option. The photopaper's discoloration is visually interpretable without additional testing providing communities can access or build a makeshift darkroom. We have successfully field tested fixing samples in a homemade darkroom.

Photopaper monitoring unlike monitoring with digital device, could make the QA/QC practices more accessible for communities. As community members place their own devices including blanks and field duplicates, they engage in QA/QC to ensure data reliability. Rather than merely creating more work, this approach enables communities to understand data reliability and potentially evaluate, rather than simply receive, data.

Relying on XRF to assess H_2S concentration would make the tool less accessible to communities as it increases the cost by ~$35 per sample. However, it is a feasible next step for communities to take if they find significant photopaper discoloration and have access to a small quantity of funding along with university partners. To overcome these limitations, we focused on developing a regression model and colorimetric concentration curve to estimate atmospheric sulfur concentrations as discussed below.

Discoloration of the photopaper reliably correlates with H_2S concentrations. As the grayscale values correlate with estimated H_2S concentrations, we believe it will be possible to further develop the colorimetric scale for estimating the concentration of H_2S. Such a scale will need to account for time, as discoloration varies with time and H_2S concentration. Next, we will develop an RGB and grayscale machine learning model for estimating H_2S concentration. Such a model could enable a phone application for taking a photograph of a sample, assessing its exposure time, color and luminance to predict the H_2S concentration (Castner et al., 2018). Additionally, the model could be used to predict a colorimetric scale for concentration over time that could be used without a phone.

Integrative scale for Corrosion and H_2S concentration. ISA corrosion classification also enables the development of a colorimetric scale for estimating corrosion. As the CCCs classify H_2S above 50 ppb as severe corrosion all our CCCs were severely corroded and as the detection limit for the photopaper is 30 ppb any perceptible discoloration of the photopaper is likely an indicator of severely corrosive conditions by the ISA scale. This scale is designed for indoor use and there may be more appropriate corrosion scales for outdoor conditions.

Collective Efficacy and Actionable Data. The design of this colorimetric scale we hope will increase community collective efficacy and create actionable data. First, based on our sewage treatment plant studies, we add benchmarks to the scale for a location where H_2S is regulated, routinely monitored and emissions managed. Communities could compare their finding to these averages, potentially enabling them to argue more effectively for similar protection to those found in workplace contexts including training in H_2S safety, alarms, personal monitors, and scrubbing of emissions.

Second, by employing photopaper as an integrated measure for corrosion we enable evaluation of property damage through corrosion. Anecdotally, communities report increased corrosion and property damage associated with smelling H_2S. This scale could allow communities to make claims about damage to physical property before that property is severely damaged, just as CCCs allow industrial users to do in workplaces (such as computers in paper pulp mills). Additionally, property damage claims may be easier for communities to make than health-based claims, which are notoriously challenging to prove particularly when symptoms are nonspecific (Allen, 2003).

Third, we imagine that individuals increase collective efficacy by sharing their results on this scale with others in their community so as to build recognition of H_2S exposures as a shared problem. Additionally, the tool can be used to map large areas to illustrate shared exposure landscapes (Wylie et al., 2017; Horwell et al., 2004, 2005). Finally, communities could add benchmarks to this scale over time to compare H_2S exposure across regions of oil and gas extraction or different industries and thereby build connections across exposed communities.

We hope this somewhat unusual approach to method development evolved by anthropologists and sociologists of science, exposure scientists, concerned community members, artists and designers offers a different, more community-centered approach to scientific tool development that focuses on enabling community-level work to address immediate concerns of frontline communities.

Funding

This work was supported by JPB Environmental Health Fellowship award granted by The JPB Foundation and managed by the Harvard School of Public Health and the National Institute of Environmental Health Sciences of the National Institutes of Health under Award Number T32ES023769. The content is solely the responsibility of the authors and does not necessarily represent the official views of the National Institutes of Health.

Declaration of competing interest

The authors declare that they have no known competing financial interests or personal relationships that could have appeared to influence the work reported in this paper.

Acknowledgements

We extend our thanks to all the members in the Wylie lab who have been involved in making photopaper samplers, assisted with field testing and data entry, particularly Kaline Langley (undergraduate student Northeastern Biology/Journalism major) for her excellent work making and scanning the photographic paper and Erik Hanley for assisting with the June 2017 field work. Additionally, the work of Rebecca Elliot (Northeastern Undergraduate Health Science Major) and Larissa Aiko Morikawa (Northeastern Undergraduate Health Science Major) preparing grayscale values was extremely valuable. We send thanks to Deb Thomas who coordinated the field work Wyoming, to Megan McLaughlin who first mapped the Wyoming data and the Wyoming landowners with whom we worked. In advising the development of the project we extend thanks to JPB Fellows who provided input on the development of this method during numerous fellows meetings, to Jack Spengler JPB Fellowship director and advisor to this project, Prof. Joseph Allen for his advice on the Corrosion Coupons and Dr. Robin Dodson at the Silent Spring Institute for her steadfast advice on study design. Additionally, we offer thanks to Prof. Christofer Leygraf who generously provided an outside review of the paper prior to submission. We extend our thanks to the Sewage Treatment Plant staff and scientists for hosting us for this study in an amazing example of public infrastructure supporting citizen science. This work would not have been possible without the support of the JPB Environmental Health Fellowship through the JPB Foundation. Additionally, we thank the Public Lab community where development of this method first began while Dr. Wylie directed their Toxics and Health Research program, particularly Shannon Dosemagen and Gretchen Gehkre. Finally we extend thanks to Northeastern's Social Science Environmental Health Research Institute (SSEHRI) who reviewed drafts of this paper and particularly the graduate students who also assisted in data analysis: Elisabeth Wilder for supporting field research in Wyoming, Mia Renauld for her support with field research at the sewage treatment plant, and Taylor Braswell for gathering Wyoming weather data. We extend our deepest gratitude to Bruce Hamilton, the Media Services Manager at Northeastern University, who gave us access to the university darkroom.

Appendix A. Supplementary data

Supplementary data to this article can be found online at https://doi.org/10.1016/j.aeaoa.2019.100049.

Appendix 1

Location	Parameter	Min.	Median	Mean	Max.	SD	Duplicate p-value for Silver	Duplicate p-value for Sulfur	Duplicate p-alue for Grayscale	Duplicate p-value for CCCs	Blankp-value for Silver	Blank p-value for Sulfur	Blank p-value for Grayscale	Blank p-value of CCCs
All Samples	Jerome H_2S (ppb)	NA	NA	NA	NA	NA	NA	NA	NA	NA	NA	NA	NA	NA
	Predicted H_2S (ppb)	-40.97	41.78	120.32	451.81	1542.01	0.71	0.78	0.49	0.69	0.29	0.29	0.29	0.67
	Silver (μg/filter)	47.46	798.53	1348.56	8145.83	139.17	0.71	0.78	0.49	0.69	0.29	0.29	0.29	0.67
	Sulfur (μg/filter)	76.44	118.95	176.38	731.21	48.79	0.71	0.78	0.49	0.69	0.29	0.29	0.29	0.67
	grayscale (GIMP units/filter)	41.50	101.20	116.42	220.80	164.48	0.71	0.78	0.49	0.69	0.29	0.29	0.29	0.67
Sewage Treatment Plant, All Rounds	Jerome H_2S (ppb)	NA	NA	NA	NA	NA	NA	NA	NA	NA	NA	NA	NA	NA
	Predicted H_2S (ppb)	-28.57	273.84	235.59	451.81	850.43	0.74	1.00	0.74	0.69	0.40	0.40	0.40	0.67
	Silver (μg/filter)	47.46	619.15	940.29	2872.46	77.99	0.74	1.00	0.74	0.69	0.40	0.40	0.40	0.67
	Sulfur (μg/filter)	82.55	133.10	165.69	335.24	58.41	0.74	1.00	0.74	0.69	0.40	0.40	0.40	0.67
	grayscale (GIMP units/filter)	41.50	117.45	127.33	217.90	171.83	0.74	1.00	0.74	0.69	0.40	0.40	0.40	0.67
Sewage Treatment Plant August 2018	Jerome H_2S (ppb)	0.00	223.5	301.54	861.70	260.83	NA	NA	NA	NA	NA	NA	NA	NA
	Predicted H_2S (ppb)	112.78	372.12	346.26	451.81	940.98	0.92	0.77	0.77	0.31	0.50	0.50	0.50	0.67
	Silver (μg/filter)	102.16	176.31	195.40	335.24	83.25	0.92	0.77	0.77	0.31	0.50	0.50	0.50	0.67
	Sulfur (μg/filter)	206.00	1030.39	1232.93	2872.46	64.32	0.92	0.77	0.77	0.31	0.50	0.50	0.50	0.67
	grayscale (GIMP units/filter)	42.90	141.05	138.15	217.90	106.57	0.92	0.77	0.77	0.31	0.50	0.50	0.50	0.67
Sewage Treatment Plant June 2017	Jerome H_2S (ppb)	NA	NA	NA	NA	NA	NA	NA	NA	NA	NA	NA	NA	NA
	Predicted H_2S (ppb)	-28.57	50.99	51.12	134.22	345.22	0.84	0.69	0.44	1.00	1.00	1.00	1.00	1.00
	Silver (μg/filter)	47.46	384.16	452.56	1048.48	32.65	0.84	0.69	0.44	1.00	1.00	1.00	1.00	1.00
	Sulfur (μg/filter)	82.55	109.18	116.17	175.72	46.51	0.84	0.69	0.44	1.00	1.00	1.00	1.00	1.00
	grayscale (GIMP units/filter)	41.50	108.15	109.28	176.00	52.94	0.84	0.69	0.44	1.00	1.00	1.00	1.00	1.00
Deaver, All Rounds	Jerome H_2S (ppb)	NA	NA	NA	NA	NA	NA	NA	NA	NA	NA	NA	NA	NA
	Predicted H_2S (ppb)	-40.97	0.62	52.01	426.11	1805.67	1.00	1.00	1.00	NA	0.67	0.67	0.67	NA
	Silver (μg/filter)	151.34	859.36	1590.49	8145.83	166.33	1.00	1.00	1.00	NA	0.67	0.67	0.67	NA
	Sulfur (μg/filter)	76.44	101.32	182.71	731.21	41.95	1.00	1.00	1.00	NA	0.67	0.67	0.67	NA
	grayscale (GIMP units/filter)	71.90	95.50	109.96	220.80	116.82	1.00	1.00	1.00	NA	0.67	0.67	0.67	NA

(*continued on next page*)

(*continued*)

Location	Parameter	Min.	Median	Mean	Max.	SD	Duplicate p-value for Silver	Duplicate p-value for Sulfur	Duplicate p-alue for Grayscale	Duplicate p-value for CCCs	Blankp-value for Silver	Blank p-value for Sulfur	Blank p-value for Grayscale	Blank p-value of CCCs
Deaver, July 31-August 22, 2013 (23 Days)	Jerome H_2S (ppb)	NA	NA	NA	NA	NA	NA	NA	NA	NA	NA	NA	NA	NA
	Predicted H_2S (ppb)	-8.28	27.89	76.22	335.29	2177.73	NA	NA	NA	NA	NA	NA	NA	NA
	Silver (μg/filter)	562.93	1612.07	2362.40	8145.83	204.46	NA	NA	NA	NA	NA	NA	NA	NA
	Sulfur (μg/filter)	85.39	153.38	244.23	731.21	47.13	NA	NA	NA	NA	NA	NA	NA	NA
	grayscale (GIMP units/filter)	81.60	119.05	131.01	220.80	108.77	NA	NA	NA	NA	NA	NA	NA	NA
Deaver, July 31-August 7, 2013 (8 Days)	Jerome H_2S (ppb)	NA	NA	NA	NA	NA	NA	NA	NA	NA	NA	NA	NA	NA
	Predicted H_2S (ppb)	-40.97	-10.41	25.94	426.11	694.85	NA	NA	NA	NA	NA	NA	NA	NA
	Silver (μg/filter)	151.34	554.34	759.21	2813.68	74.06	NA	NA	NA	NA	NA	NA	NA	NA
	Sulfur (μg/filter)	76.44	94.72	116.46	355.81	18.23	NA	NA	NA	NA	NA	NA	NA	NA
	grayscale (GIMP units/filter)	71.90	83.80	87.28	141.00	123.82	NA	NA	NA	NA	NA	NA	NA	NA

Appendix 2

Parameter	Location	Min.	Median	Mean	Max.
Humidity	All Samples	10.00	61.53	60.23	100.00
	Deaver, July 31-August 7, 2013 (8 Days)	20.00	53.00	56.74	100.00
	Deaver, July 31-August 22, 2013 (23 Days)	10.00	42.00	44.31	100.00
	Sewage Treatment Plant, All Samples	31.51	64.32	65.13	86.69
	Sewage Treatment Plant June 2017	40.65	60.00	59.39	75.18
	Sewage Treatment Plant, August 2018	31.51	72.13	70.76	86.69
Temperature	All Samples	52.00	73.99	73.80	95.00
	Deaver, July 31-August 7, 2013 (8 Days)	54.00	68.00	67.84	90.00
	Deaver, July 31-August 22, 2013 (23 Days)	52.00	70.00	70.21	95.00
	Sewage Treatment Plant, All Samples	60.43	74.73	74.90	90.38
	Sewage Treatment Plant June 2017	60.43	71.75	71.82	82.98
	Sewage Treatment Plant, August 2018	71.49	78.43	77.93	90.38

Appendix 3

Photopaper ID	SG.2.2FB	SG.1.1a	SG.2.1b	SG.2.2a	SG.3.1a	SG.4.1b
Time (days)	2	1	2	2	3	4
Silver (μg/filter/h)	-0.01	8.37	13.45	16.57	17.47	19.11
Sulfur (μg/filter/h)	-1.12	9.60	43.65	57.68	109.83	162.82
Greyscale	0.80	42.90	106.40	119.80	162.30	191.90
H_2S (ppb/h)	-11.53	102.89	249.62	333.76	425.77	473.94

References

Agyeman, J., Schlosberg, D., Craven, L., Matthews, C., 2016 Nov. Trends and directions in environmental justice: From inequity to everyday life, community, and just sustainabilities. Annu. Rev. Environ. Resour. 41 (1), 321–340.

Allen, B.L., 2003. Uneasy Alchemy: Citizens and Experts in Louisiana's Chemical Corridor Disputes. MIT Press, Cambridge, MA.

Allen, J.G., MacIntosh, D.L., Saltzman, L.E., Baker, B.J., Matheson, J.M., Recht, J.R., et al., 2012. Elevated corrosion rates and hydrogen sulfide in homes with 'Chinese drywall'. Sci. Total Environ. 426, 113–119.

Asbestos Air, 2019. 25mm PCM 0.8; asbestos air monitoring cassette | environmental monitoring systems [Internet]. [cited 2019 May 1]. Available from: https://www.emssales.net/cassettes-supplies/asbestos/cassettes/25mm-pcm-0-8-mu-asbestos-air-monitoring-cassette.html.

Arizona Instruments, LLC, 2015. User manual: Jerome® J605 hydrogen sulfide analyzer [Internet], [cited 2017 May 12]. Available from: http://www.azic.com/jerome/j605/.

ASHRAE, P., 2014. Gaseous Contamination in Datacom Environments. American Society of Heating, Refrigerating and Air-Conditioning Engineers.

Bandura, A., 1997. Self-Efficacy: The Exercise of Control. W.H. Freeman and Company, New York.

Bandura, A., 2000 Jun 1. Exercise of human agency through collective efficacy. Curr. Dir. Psychol. Sci. 9 (3), 75–78.

Brody, J.G., Morello-Frosch, R., Zota, A., Brown, P., Pérez, C., Rudel, R.A., 2009. Linking exposure assessment science with policy objectives for environmental justice and breast cancer advocacy: The Northern California Household Exposure Study. Am. J. Public Health 99 (S3), S600–S609.

Brody, J.G., Dunagan, S.C., Morello-Frosch, R., Brown, P., Patton, S., Rudel, R.A., 2014. Reporting individual results for biomonitoring and environmental exposures: Lessons learned from environmental communication case studies. Environ. Health 13 (1), 40.

Brown, P., Zavestoski, S., McCormick, S., Mayer, B., Morello-Frosch, R., Gasior Altman, R., 2004 Jan. Embodied health movements: New approaches to social movements in health. Sociol. Health Illn. 26 (1), 50–80.

Brown, P., Zavestoski, S., Cordner, A., McCormick, S., Mandelbaum, J., Luebke, T., et al., 2011. A Narrowing Gulf of Difference? Disputes and Discoveries in the Study of Gulf War–Related Illnesses. In: Contested Illnesses: Citizens, Science, and Health Social Movements. University of California Press, Berkeley, pp. 79–107.

Browning, C.R., Burrington, L.A., Leventhal, T., Brooks-Gunn, J., 2008. Neighborhood structural inequality, collective efficacy, and sexual risk behavior among urban youth. J. Health Soc. Behav. 49 (3), 269–285.

Bullard, R.D., 2008. Dumping in Dixie: Race, Class, and Environmental Quality, third ed. Westview Press, New York, NY.

Carpenter, T.S., Rosolina, S.M., Xue, Z.-L., 2017 Dec. Quantitative, colorimetric paper probe for hydrogen sulfide gas. Sens. Actuators B Chem. 253, 846–851.

Castner, J., Gehrke, G.E., Shapiro, N., Dannemiller, K.C., 2018. Community interest and feasibility of using a novel smartphone-based formaldehyde exposure detection technology. Public Health Nurs. 35 (4), 261–272.

Purafil, Inc.. CCC (Corrosion Classification Coupon)[Internet]. Purafil. [cited 2019 May 1]. Available from: https://www.purafil.com/products/monitoring/passive-monitoring/ccc/.

Clough, E., 2018. Environmental justice and fracking: A review. Curr. Opin. Environ. Sci. Health 3, 14–18.

Cohen, D.A., Inagami, S., Finch, B., 2008. The built environment and collective efficacy. Health Place 14 (2), 198–208.

Contributors from Public Lab, 2018. Hydrogen Sulfide Photopaper [Internet]. Public Lab. [cited 2019 May 1]. Available from: publiclab.org/n/15478.

Corburn, J., 2005. Street Science: Community Knowledge and Environmental Health Justice. MIT Press, Cambridge, MA.

Eriksen, M., Liboiron, M., Kiessling, T., Charron, L., Alling, A., Lebreton, L., et al., 2018. Microplastic sampling with the AVANI trawl compared to two neuston trawls in the Bay of Bengal and South Pacific. Environ. Pollut. 232, 430–439.

Fagan, A.A., Wright, E.M., Pinchevsky, G.M., 2014. The protective effects of neighborhood collective efficacy on adolescent substance use and violence following exposure to violence. J. Youth Adolesc. 43 (9), 1498–1512.

FB6280E. Best solution for book scanning [Internet]. Avision. [cited 2019 May 1]. Available from: https://www.avision.com/motion.asp?lgid=2&menuid=10075&prodid=121298&cat=13.

Finnbjornsdottir, R.G., Carlsen, H.K., Thorsteinsson, T., Oudin, A., Lund, S.H., Gislason, T., et al., 2016. Association between daily hydrogen sulfide exposure and incidence of emergency hospital visits: a population-based study. PLOS ONE 11 (5), e0154946.

Freire, P., 1968. Pedagogy of the Oppressed. Seabury Press, New York.

Goddard, R.D., Hoy, W.K., Hoy, A.W., 2004. Collective efficacy beliefs: Theoretical developments, empirical evidence, and future directions. Educ. Res. 33 (3), 3–13.

Hamoda, M.F., 2006 Jan. Air pollutants emissions from waste treatment and disposal facilities. J. Environ. Sci. Health Part A 41 (1), 77–85.

Han, T., Coles, H., Price, P.N., Gadgil, A., Tschudi, W., 2019. Corrosion Coupons May Not Be Useful for Predicting Data Center Equipment Failure Rates. International Society of Indoor Air Quality and Climate. https://www.isiaq.org/docs/presentations/0997_Han.pdf. (Accessed 10 April 2019).
Hess, D.J., 2016. Undone Science: Social Movements, Mobilized Publics, and Industrial Transitions [Internet]. MIT Press, Cambridge, MA. Available from: https://muse.jhu.edu/book/48162.
Histogram Dialog, 2019. Gimp [Internet], [cited 2019 May 1]. Available from: https://docs.gimp.org/2.10/en/gimp-histogram-dialog.html.
Horwell, C.J., Allen, A.G., Mather, T.A., Patterson, J.E., 2004. Evaluation of a novel passive sampling technique for monitoring volcanogenic hydrogen sulfide. J. Environ. Monit. 6 (7), 630–635.
Horwell, C.J., Patterson, J.E., Gamble, J.A., Allen, A.G., 2005. Monitoring and mapping of hydrogen sulphide emissions across an active geothermal field: Rotorua, New Zealand. J. Volcanol. Geotherm. Res. 139 (3), 259–269.
Hydrogen sulfide test Kit, model HS-C [Internet]. HACH USA. [cited 2019 May 1]. Available from: https://www.hach.com/hydrogen-sulfide-test-kit-model-hs-c/product?id=7640219546.
Kenny, C., Liboiron, M., Wylie, S.A., 2019. Seeing power with a flashlight: DIY thermal sensing technology in the classroom. Soc. Stud. Sci. 49 (1), 3–28.
Kilburn, K.H., 2012. Human impairment from living near confined animal (hog) feeding operations [Internet] J. Environ. Public. Health [cited 2017 May 12];2012. Available from: https://www.hindawi.com/journals/jeph/2012/565690/abs/.
Kilburn, K.H., Warshaw, R.H., 1995. Hydrogen sulfide and reduced-sulfur gases adversely affect neurophysiological functions. Toxicol. Ind. Health 11 (2), 185–197.
Kilburn, K.H., Thrasher, J.D., Gray, M.R., 2010. Low-level hydrogen sulfide and central nervous system dysfunction. Toxicol Ind Health [Internet], [cited 2017 May 12]; Available from: http://tih.sagepub.com/content/early/2010/05/05/0748233710369126.
Kim, H., 2003 Apr. Corrosion process of silver in environments containing 0.1 ppm H2S and 1.2 ppm NO2. Mater. Corros. 54 (4), 243–250.
Koch, G., Varney, J., Thompson, N., Moghissi, O., Gould, M., Payer, J., 2016. International measures of prevention, application, and economics of corrosion technologies study. NACE Int.
Kodak Photo Flo 200 - 16 oz. Freestyle photographic supplies [Internet], [cited 2019 May 1]. Available from: https://www.freestylephoto.biz/1464510-Kodak-Photo-Flo-200-16-oz.
Kornblug, S., 2014. Sensing Hydrogen Sulfide from CAFO Emissions in Poweshiek County [Internet]. Public Lab: a DIY environmental Science Community, Iowa. Available from: https://publiclab.org/notes/sophie/07-16-2014/sensing-hydrogen-sulfide-from-cafo-emissions-in-poweshiek-county-iowa.
Latour, B., 1987. Science in Action: How to Follow Scientists and Engineers through Society. Harvard University Press, Cambridge, MA.
Latour, B., Woolgar, S., 1986. Laboratory Life: The Construction of Scientific Facts. Princeton University Press, Princeton, NJ.
Legator, M.S., Singleton, C.R., Morris, D.L., Philips, D.L., 2001. Health effects from chronic low-level exposure to hydrogen sulfide. Arch. Environ. Health 56 (2), 123–131.
Leygraf, C., Wallinder, I.O., Tidblad, J., Graedel, T., 2016. Atmospheric Corrosion. John Wiley & Sons, New York, NY.
Liboiron, M., 2017 Sep 28. Compromised agency: The case of BabyLegs. Engag. Sci. Technol. Soc. 3, 499.
Macey, G.P., Breech, R., Chernaik, M., Cox, C., Larson, D., Thomas, D., et al., 2014. Air concentrations of volatile compounds near oil and gas production: A community-based exploratory study. Environ. Health 13 (1), 82.
Malin, S.A., DeMaster, K.T., 2016. A devil's bargain: Rural environmental injustices and hydraulic fracturing on Pennsylvania's farms. J. Rural Stud. 47, 278–290.
Markowitz, G., Rosner, D., 2013. Deceit and Denial: The Deadly Politics of Industrial Pollution. University of California Press, Oakland, CA, p. 446.
Matz, J.R., Wylie, S., Kriesky, J., 2017. Participatory air monitoring in the midst of uncertainty: Residents' experiences with the Speck Sensor. Engag. Sci. Technol. Soc. 3, 464–498.
Minkler, M., Wallerstein, N., 2008. Community-based Participatory Research for Health: From Process to Outcomes, second ed. Jossey-Bass, San Francisco, CA.
Murphy, M., 2006. Sick Building Syndrome and the Problem of Uncertainty: Environmental Politics, Technoscience, and Women Workers. Duke University Press, Durham, NC.
Natusch, D.F.S., Sewell, J.R., Tanner, R.L., 1974 Mar. Determination of hydrogen sulfide in air. Assessment of impregnated paper tape methods. Anal. Chem. 46 (3), 410–415.
Nicole, W., 2013. CAFOs and Environmental Justice: The Case of North Carolina. National Institute of Environmental Health Sciences.
Oreskes, N., Conway, E.M., 2011. Merchants of Doubt: How a Handful of Scientists Obscured the Truth on Issues from Tobacco Smoke to Global Warming. Bloomsbury Publishing USA, New York.
Ottinger, G., 2010 Mar 1. Buckets of resistance: Standards and the effectiveness of citizen science. Sci. Technol. Hum. Values 35 (2), 244–270.
Pal, T., Ganguly, A., Maity, D.S., 1986. Use of a silver-gelatin complex for the microdetermination of hydrogen sulphide in the atmosphere. Analyst 111 (6), 691.
Pellow, D., 2016. Toward a critical environmental justice studies: Black lives matter as an environmental justice challenge. Du. Bois Rev. Soc. Sci. Res. Race 13 (2), 221–236.
People of Color Environmental Justice Summit, 1991. Principles of Environmental Justice.
Public Lab. Public Lab: a DIY environmental science community [Internet]. [cited 2019 Mar 7]. Available from: https://publiclab.org/.
Pulido, L., 2017. Geographies of race and ethnicity II: Environmental racism, racial capitalism and state-sanctioned violence. Prog. Hum. Geogr. 41 (4), 524–533. May 13.
Pulido, L., 2018 Apr 1. Geographies of race and ethnicity III: Settler colonialism and nonnative people of color. Prog. Hum. Geogr. 42 (2), 309–318.
Purafil, Inc., 2017. Causes of Corrosion and Corrosion Monitoring. Purafil, Inc. [cited 2019 May 1] Available from: https://www.purafil.com/causes-corrosion-corrosion-monitoring/
Purafil, Inc., 2017. ISA Environmental Classifications: Changes and New Requirements. Purafil, Inc. [cited 2019 Apr 10] Available from: https://www.purafil.com/isa-environmental-classifications-changes-new-requirements/
Quddious, A., Yang, S., Khan, M., Tahir, F., Shamim, A., Salama, K., et al., 2016. Disposable, paper-based, inkjet-printed humidity and H2S gas sensor for passive sensing applications. Sensors 16 (12), 2073.
RECORD Speed Fixer, 2018. Sprint Systems of Photography [Internet] [cited 2019 May 1]. Available from: https://sprintsystems.com/product/record-speed-fixer/.
Rice, D.W., Peterson, P., Rigby, E.B., Phipps, P.B.P., Cappell, R.J., Tremoureux, R., 1981. Atmospheric corrosion of copper and silver. J. Electrochem. Soc. 128 (2), 275–284.
Richter, L., Cordner, A., Brown, P., 2018 Oct 1. Non-stick science: Sixty years of research and (in)action on fluorinated compounds. Soc. Stud. Sci. 48 (5), 691–714.
Rosolina, S.M., Carpenter, T.S., Xue, Z.-L., 2016 Feb 2. Bismuth-based, disposable sensor for the detection of hydrogen sulfide gas. Anal. Chem. 88 (3), 1553–1558.
Sampson, R.J., Raudenbush, S.W., Earls, F., 1997. Neighborhoods and violent crime: A multilevel study of collective efficacy. Science 277 (5328), 918–924.
Sanderson, H.P., Thomas, R., Katz, M., 1966 Jun 1. Limitations of the lead acetate impregnated paper tape method for hydrogen sulfide. J. Air Pollut. Control Assoc. 16 (6), 328–330.
Saxton, D.I., 2015. Strawberry fields as extreme environments: The ecobiopolitics of farmworker health. Med. Anthropol. 34 (2), 166–183.
Shapiro, N., 2015. Attuning to the chemosphere: Domestic formaldehyde, bodily reasoning, and the chemical sublime. Cult. Anthropol. 30 (3), 368–393.
Skrtic, L., 2006. Hydrogen Sulfide, Oil and Gas, and People's Health. Diplom Rad Berkeley Univ Calif.
Thomas, D., 2014. Breathe at Your Own Risk. Unpublished Report on Wyoming Community Monitoring.
Thomas, D., 2017. Living with oil and gas and practicing community conducted science. Engag. Sci. Technol. Soc. 3, 613–618.
Van Meel, K., Smekens, A., Behets, M., Kazandjian, P., Van Grieken, R., 2007. Determination of platinum, palladium, and rhodium in automotive catalysts using high-energy secondary target X-ray fluorescence spectrometry. Anal. Chem. 79 (16), 6383–6389.
Van Meel, K., Fontas, C., Van Grieken, R., Queralt, I., Hidalgo, M., Marguí, E., 2008. Application of high-energy polarised beam energy dispersive X-ray fluorescence spectrometry to cadmium determination in saline solutions. J. Anal. At. Spectrom 23 (7), 1034–1037.
Venturi, S., Cabassi, J., Tassi, F., Capecchiacci, F., Vaselli, O., Bellomo, S., et al., 2016 Sep. Hydrogen sulfide measurements in air by passive/diffusive samplers and high-frequency analyzer: A critical comparison. Appl. Geochem. 72, 51–58.
Vogel, S.A., 2012. Is it Safe? BPA and the Struggle to Define the Safety of Chemicals. University of California Press, Berkeley, CA.
Wilson, S.M., Howell, F., Wing, S., Sobsey, M., 2002. Environmental injustice and the Mississippi hog industry. Environ. Health Perspect. 110 (2), 195–201.
Wing, S., 1994. Limits of epidemiology. Med. Glob. Surviv. 1 (2), 74–86.
Wing, S., 1998. Whose epidemiology, whose health? Int. J. Health Serv. 28 (2), 241–252.
Wylie, S., 2018. Fractivism: Corporate Bodies and Chemical Bonds. Duke University Press, Durham, NC.
Wylie, S., Albright, L., 2014. WellWatch: Reflections on designing digital media for multi-sited para-ethnography. J. Polit. Ecol. 21 (1), 321–348.
Wylie, S.A., Jalbert, K., Dosemagen, S., Ratto, M., 2014 Mar. Institutions for civic technoscience: How critical making is transforming environmental research. Inf. Soc. 30 (2), 116–126.
Wylie, S., Shapiro, N., Liboiron, M., 2017 Sep 28. Making and doing politics through grassroots scientific research on the energy and petrochemical industries. Engag Sci Technol. Soc. 3 (0), 393–425.
Wylie, S., Wilder, E., Vera, L., Thomas, D., McLaughlin, M., 2017. Materializing exposure: Developing an indexical method to visualize health hazards related to fossil fuel extraction. Engag. Sci. Technol. Soc. 3, 426–463.
Yang, C.J., Liang, C.H., Liu, X., 2007. Tarnishing of silver in environments with sulphur contamination. Anti-Corros. Methods Mater. 54 (1), 21–26.